Late Pliocene – early Pleistocene deep-sea basin sedimentation at high-latitudes; mega-scale submarine slides of the north-western Barents Sea margin prior to the shelf-edge glaciations

Safronova, P.A.,*[1, 2] Laberg, J.S., [1, 3] Andreassen, K., [4, 1], Shlykova, V.[5], Vorren, T.O.[†], [1] and Chernikov, S.[5]

* Corresponding author: Polina Alekseevna Safronova; e-mail address:

polina.a.safronova@gmail.com; polina.safronova@gdfsuezep.no; tel. mob.: (+47) 41077566.

[1] Department of Geology, the Faculty of Science and Technology, the Arctic University of Norway; Dramsveien 201, 9037-Tromsø, Norway

[2] Now at: GDF SUEZ E&P Norge AS, Vestre Svanholmen 6, Sandnes, Norway

[3] Also at: Research Centre for Arctic Petroleum Exploration (ARCEx), Department of Geology, the Arctic University of Norway, N-9037 Tromsø, Norway

[4] Centre of Excellence for Arctic Gas Hydrate, Environment and Climate (CAGE), the Arctic University of Norway, Tromsø.

[5] Russian Joint Stock Company “Marine Arctic Geological Expedition”; Sofia Perovskaya Str., 26, 183012-Murmansk, Russian Federation

[†] Passed away 16.06.2013

Keywords: Submarine slides, Barents Sea, passive and glaciated continental margin, sedimentary processes, debrite, Storfjorden TMF, Kveitola TMF

Abstract

At high-latitude continental margins, large-scale submarine sliding has been an important process for deep-sea sediment transfer during glacial and interglacial periods. Little is however known about the importance of this process prior to the arrival of the ice sheet on the continental shelf. Based on new two-dimensional seismic data from the NW Barents Sea continental margin, this study documents the presence of thick and regionally extensive submarine slides formed between 2.7 and 2.1 Ma, before shelf-edge glaciation. The largest submarine slide, located in the northern part of the Storfjorden Trough Mouth Fan (TMF), left a scar and is characterized by an at least 870 m thick interval of chaotic to reflection-free seismic facies interpreted as debrites. The full extent of this slide debrite 1 is yet unknown but it has a mapped areal distribution of at least 10.7×10^3 km^2 and it involved > 4.1×10^3 km^3 of sediments. It remobilized a larger sediment volume than one of the largest exposed submarine slides in the world – the Storegga Slide in the Norwegian Sea. In the southern part of the Storfjorden TMF and along the Kveithola TMF, the seismic data reveal at least four large-scale slide debrites, characterized by seismic facies similar to the slide debrite 1. Each of them is ca. 295 m thick, covers an area of at least 7.04×10^3 km^2 and involved $1,1\times10^3$ km^3 of sediments. These five submarine slide debrites represent approximately one quarter of the total volume of sediments deposited during the time 2.7-1.5 Ma along the NW Barents Sea.

The preconditioning factors for submarine sliding in this area probably included deposition at high sedimentation rate, some of which may have occurred in periods of low eustatic sea-level. Intervals of weak contouritic sediments might also have contributed to the instability of part of the slope succession as these deposits are known from other parts of the Norwegian margin and elsewhere to have the potential to act as weak layers. Triggering was probably caused by seismicity associated with the nearby and active Knipovich spreading ridge and/or the old tectonic lineaments within the Spitsbergen Shear Zone. This seismicity is inferred to be the main influence of the large-scale sliding in this area as this and previous studies have documented that sliding have occurred independently of climatic variations, i.e. both before and during the period of ice sheets repeatedly covering the continental shelf.

1. Introduction

A growing amount of literature has been dedicated to deep-water basin sedimentation and its control along high-latitude (north of 52°N) and glaciated continental margins (e.g. Vorren *et al.*, 1998; Dowdeswell & Cofaigh, 2002; Dahlgren *et al.*, 2005; Laberg *et al.*, 2012). Some of the most detailed work has been conducted in the Polar North Atlantic due to the presence of extensive geological and geophysical data (e.g. Faleide *et al.*, 1996; Hjelstuen *et al.*, 1996; Vorren & Laberg, 1997). However, the importance of deep-water sedimentation processes before shelf-edge glaciation at these high-latitude continental margins has barely been addressed. This includes the occurrence, frequency and origin of large-scale submarine landslides prior the first arrival of the ice sheet at the shelf edge.

Over the last ca. 1.5 Ma, a period during which grounded ice sheets repeatedly reached the shelf break along the Norwegian – Barents Sea – Svalbard continental margin, a relatively high number of large-scale submarine slides have occurred. This includes the northern Svalbard margin (Vanneste et al., (2006), the NW Barents Sea margin (Lucchi *et al.*, 2012; Rebesco *et al.*, 2012) and the SW Barents Sea margin (Laberg & Vorren, 1993; Kuvaas & Kristoffersen, 1996; Hjelstuen *et al.*, 2007). Similar features have also been identified offshore mainland Norway (Bugge, 1983; Laberg & Vorren, 2000; Laberg *et al.*, 2000; Laberg *et al.*, 2002; Haflidason *et al.*, 2004; Lindberg *et al.*, 2004). The Storegga Slide (Haflidason *et al.*, 2004) and the Bjørnøya Fan Slide Complex ((Hjelstuen *et al.*, 2007), which have occurred offshore mainland Norway and the SW Barents Sea respectively, are among the largest events reported worldwide (Hjelstuen *et al.*, 2007).

It is important to study submarine slides and to be able to predict preconditioning factors of their failure, because they play an essential role in the transfer of sediment into the deep-water and consequently deliver a significant part of the sedimentary basin fill (e.g. Moscardelli & Wood, 2008). They may also have a profound influence on the post-failure continental margin sedimentation as slide scars may act as sediment traps for contouritic sediments transported by ocean currents (Laberg *et al.*, 2001; Laberg & Camerlenghi, 2008). In addition, a sudden displacement of the sea-floor through catastrophic sediment failure can affect offshore infrastructure (cables, pipelines and platforms) and disrupt the water column above the failure generating a tsunami that could affect coastal areas and cause loss of human life (e.g. Canals *et al.*, 2004; Hjelstuen *et al.*, 2007; Leynaud *et al.*, 2009; Mosher *et al.*, 2010).

In this study, newly available high-resolution two-dimensional seismic data from the Russian Joint Stock Company "Marine Arctic Geological Expedition" are used to present the first detailed description and discussion of deep-water sedimentation processes in the NW Barents Sea area with special focus on large-scale submarine slides prior the first arrival of the ice sheet at the shelf edge (Fig. 1).

2. Geological setting

The study area is located on the passive continental margin of the north-western Barents Sea and south-western Svalbard, where the water depth is between 350m and 2500m. The most prominent geomorphological features in the study area are the Storfjorden, Kveithola and Bellsund Trough Mouth Fans (TMFs) developed at the mouth of same-name cross-shelf troughs (Fig. 1A). The continental slope is about 0.2-1.8° along the Storfjorden TMF area and 1.8-3.2° in Bellsund TMF. Tectonically, the study area corresponds to the western part of a regional continental shear zone, the Spitsbergen Shear Zone, which acted as the plate boundary between the incipient Norwegian Sea and the Arctic Ocean (Talwani & Eldholm, 1977; Crane *et al.*, 2001) (Fig. 2A). In the west the margin is delineated by the Mid-Atlantic Ridge which can be traced through Iceland into the Norwegian-Greenland Sea as the Mohns and Knipovich Ridges (Fig. 2A). The active Knipovich Ridge is located in close proximity to the continental margin of the Svalbard Archipelago (Crane *et al.*, 2001).

The Late Cenozoic depositional environment of the western Barents Sea/Svalbard margin was strongly influenced by tectonically induced uplift and Late Pliocene to Pleistocene climate deterioration and onset of Northern Hemisphere Glaciations (3.6-2.4 Ma) (e.g. Vorren *et al.*, 1991; Knies *et al.*, 2009). The established fluvial-glaciofluvial erosional and depositional regime during the Late Pliocene-Pleistocene greatly increased sedimentation rates and led to formation of prominent westward prograding wedges, TMFs, near the shelf edge in front of bathymetric troughs in the western Barents Sea - Svalbard area (e.g. Faleide *et al.*, 1996; Hjelstuen *et al.*, 1996; Vorren *et al.*, 1998; Dahlgren *et al.*, 2005) (Fig. 1A). Climate is regarded as the main factor controlling the TMF growth, and glacially derived sediments comprise a significant proportion of the TMFs in some areas. However, it is stillunclear if the initial stage of TMF growth occurred either during a fluvial/glacifluvial phase in response to tectonically induced uplift or as a result of shelf-edge glaciations at later stage (Bugge *et al.*, 1987; Butt *et al.*, 2000; Lindberg *et al.*, 2004; Dahlgren *et al.*, 2005; Andreassen *et al.*, 2007).

Knies et al. (2009) suggested three phases of ice sheet growth in the Barents Sea-Svalbard region: (1) an initial phase between ca 3.6 Ma and 2.4 Ma characterized by short-term glacial intensification covering mountainous regions and beyond the coastline in the northern/western Barents Sea; (2) a transitional growth phase between ca. 2.4 and 1.0 Ma when the ice sheet expanded towards the southern Barents Sea; (3) the large-scale intensification of glaciation in the Barents Sea after ca. 1.0 Ma with repeated advances to the shelf edge and high frequencies of gravity-driven mass movements along the western Barents Sea margin.

The north-western Barents Sea continental margin is characterized by ca. 4000 m thick Late Pliocene-Pleistocene predominantly glaciogenic sediments forming Kveithola Trough Mouth Fan (TMF) and Storfjorden TMF - the second largest along the entire margin in terms of volume (Hjelstuen *et al.*, 1996) (Fig. 1A). It shows the maximum shelf break progradation of 50 km along the margin during a period of glacial influence (Solheim *et al.*, 1998). The Storfjorden TMF overlies both continental and oceanic crust, and forms today a broad bathymetric swell. It is located at the mouth of the east-west trending Storfjorden trough on the continental shelf and strongly related to the glaciation history of the Barents Sea-Svalbard region (Vorren *et al.*, 1989; Hjelstuen *et al.*, 1996).

Small- and large-scale submarine landslides younger than 1.0 Ma covering an area of ca. 50 km^2 to more than 1100 km^2 have been documented on the middle and upper continental slope of the NW Barents Sea margin (Lucchi *et al.*, 2012; Rebesco *et al.*, 2012). The largest shallow fan-shaped landslide, LS-1, covers an area more than 1100 km^2 along the southern Storfjorden TMF and removed approximately 33 km^3 of sediments (Rebesco *et al.*, 2012) (Fig. 2A; Table 1). Landslide 2 (LS-2) located southeast of LS-1, left a depression about 20 km long and 2 km wide, therefore covering an area of nearly 40 km^2 and removed less than 2 km^3 of sediments. The oldest landslide, PLS-1, located along the Kveithola TMF, is more than 250 m thick and has an approximate age between 1.0-0.8 Ma. The volume of sediments involved in this event is not known. Thus, no detailed estimates are available on the total volume of sediments affected by failure along this part of the margin.

To the south, on the SW Barents Sea continental margin, the large-scale Bjørnøyrenna Slide (Laberg & Vorren, 1993; 1996), the mega-scale Bjørnøya Fan Slide Complex (Hjelstuen *et al.*, 2007) and several Pliocene(?)-Pleistocene small- and large-scale slides (Knutsen *et al.*, 1992; Kuvaas & Kristoffersen, 1996) have been documented (Fig. 2A; Table 1). The 0.2-0.3 Ma old Bjørnøyrenna Slide affected an area of ca. 12.5×10^3 $km^2$and mobilized about 1100 $km^3$of sediments. The 1.0-0.2 Ma old Bjørnøya Fan Slide Complex was formed by three buried mega-failures which are up to 500 m thick each. Approximately 25000 km^3 of sediments were remobilized by each of the two largest failures. This is one order of magnitude greater than the worlds' largest exposed slide, the Storegga Slide (Hjelstuen *et al.*, 2007). In conclusion, deep-sea sediment transfer of a total volume of at least 51.1 x 10^3 km^3 of sediments has occurred on the SW Barents Sea continental margin due to sediment failure of the continental slope succession over the last ~1.5 Ma.

3. Late Cenozoic seismic stratigraphy and chronology of the western Barents Sea-Svalbard margin

Along the western Barents Sea-Svalbard margin a late Pliocene-Pleistocene seismic stratigraphic framework is established by seven regionally correlated seismic reflectors R7 (oldest) to R1 (Faleide *et al.*, 1996). Reflectors R7, R5 and R1 represent the most pronounced unconformities observed towards the shelf break and define the boundaries between three westward prograding depositional sequences GI (R7-R5), GII (R5-R1) and GIII (R1-sea floor) (Faleide *et al.*, 1996), corresponding to sequences TeC, TeD, and TeE of Vorren et al. (1991). Age constraints of the seismic stratigraphy of the western Barents Sea is mainly based on the Ocean Drilling Program (ODP) Site 986 (Fig. 1B) and exploration wells (Eidvin *et al.*, 1993; 1998; 2000; Forsberg *et al.*, 1999; Butt *et al.*, 2000; Andreassen *et al.*, 2007; Knies *et al.*, 2009), and shallow borings (Sættem *et al.*, 1992; Sættem *et al.*, 1994). R7 is the deepest reflector, which by Forsberg et al. (1999) has a tentative age of 2.3-2.4 Ma based on linear interpolation using two tie points from ~150 mbsf to ~650 mbfs. Knies et al. (2009) revised the age of R7 to ~2.7 Ma by including two additional biostratigraphic datums of ~2.41Ma at ~649 mbsf and ~2.76 Ma at ~900 mbsf. Following the same approach, Rebesco et al. (2014)

revised the ages of the younger reflectors by linear interpolation between the new datums, the Brunhes/Matuyama boundary at 133 mbsf and the top of the Jaramillo Subchron at 152 mbsf (Channel *et al.,* 1999). Therefore, the following reflectors R6, R5, R4, R3, R2 and R1 were given tentative ages of about 2.1, 1.5, 1.1, 0.75, 0.4 and 0.2Ma, respectively (Rebesco *et al.*, 2014) (Table 2). The reflector R4A was introduced during the site survey of ODP Site 986 (Jansen *et al.*, 1996), and it was given a tentative age of 1.3 Ma by Rebesco et al. (2014). Depositional sequence GI (2.7 – 1.5 Ma), bounded by reflectors R7 (oldest) and R5 is the main focus of this study.

4. Database and methods

4.1. Seismic and well data

This study has been performed by interpreting 2D seismic data of variable quality kindly provided by the Russian Joint Stock Company "Marine Arctic Geological Expedition" (MAGE) (Fig. 1B). A 2D seismic survey from the SW Svalbard margin and partly from the most northern part of the NW Barents Sea margin acquired in 2002-2004 (Fig. 1B; black lines) covers an area of approximately 16200 $km^2$and has a line spacing of roughly 11×22 km. Overall the data of a good quality. From a dominant frequency (f) of the data at the depth of target zone of 30 Hz and a seismic P-wave velocity (V) of ~2300 m/s at ODP Site 986 (Jansen *et al.*, 1996), the vertical resolution of the data is approximately 20 m (one-fourth of the dominant wavelength of the seismic pulse - $V/4f$). However, an individual unit should be at least 40 m thick (half of the dominant wavelength) to produce reflection from its top and base that do not interfere with each other. The horizontal resolution of the 2D seismic data is defined by a Fresnel zone diameter ($V/2f$ or half of the wavelength) (Brown, 1999) and is about 40 m.

Extensive 2D seismic data from the NW Barents Sea margin acquired by MAGE in 2005 and 2006 (Fig. 1B; orange and purple lines) are of variable quality and have problems with multiples, in particular, in shallow parts. They have line spacing of 10×18 km and in total cover an area of about 41000 km^2. The vertical resolution of these data at the target depth is ~ 30 m ($V/4f$), and the horizontal resolution is ~ 60 m ($V/2f$) assuming a dominant frequency of

20 Hz.

The seismic data set also includes a series of regional 2D lines acquired by MAGE in 1989-1991 (Fig. 1B; green lines), which extend across the NW Barents Sea margin and westwards into the oceanic basin. The seismic data are characterized by numerous multiples and covers a large area of about 125000 km^2. The vertical resolution at the depth of interest is about 40 m (*V/4f*) and the horizontal is ~80 m (*V/2f*) assuming a dominant frequency of 15 Hz.

Ocean Drilling Program (ODP) Site 986, drilled in 1995 at a water depth of ca. 2050 m west of Svalbard on the lower continental slope between Isfjorden and Bellsund TMFs (Jansen *et al.*, 1996; Forsberg *et al.*, 1999; Butt *et al.*, 2000) (Fig. 1B), was used in order to reveal the lithology and depositional environment of intervals of interest. Average interval velocities from the Site were used to convert measurements from seismic data in two-way travel time to meters. It allowed us to estimate thickness of the study intervals, sedimentation rates and volumes.

4.2 Study methods

Seismic stratigraphic techniques were used in order to describe and interpret individual seismic facies units within the depositional sequence GI in terms of depositional environment and lithofacies distribution (e.g. Veeken & Moerkerken, 2013). A seismic facies unit can be defined as a sedimentary unit which is different from adjacent units in its seismic characteristics such as reflection configuration, continuity, amplitude and frequency, internal geometrical relationship and external three-dimensional form (Mitchum *et al*., 1997) (Fig. 3).

The seismic reflectors R7 and R5, defining the lower and upper boundaries of the depositional sequences GI (Faleide *et al.*, 1996), were regionally correlated along the SW Svalbard-NW Barents Sea margin by using available 2D seismic data (Figs. 4A-B and 5A). In addition, regional correlation of reflector R6, recognized within the depositional sequence GI, was carried out (Figs. 4A-B and 5A). The correlation was started from ODP Site 986, which penetrated the depth of reflectors R7, R6 and R5 (Jansen *et al.,* 1996) (Fig. 4B).

During this study seismic profile A in proximity of ODP Site 986 (Fig. 1B) was used to define the location of reflectors R7, R6 and R5. It was however not possible to do a proper tie to

Site 986 due to absence of both check-shot data and parts of the wireline log data, as well as lack of velocity and density information. Therefore, a synthetic seismogram generated by Jansen et al. (1996) was used (Fig. 6A). Reflectors R7, R6 and R5 were picked on the seismic profile A at the ODP Site 986 location by selecting the closest significant reflector matching their depth (in seconds) described by Jansen et al. (1996) (Table 2; Fig. 6B). A similar approach was also taken by Rebesco et al. (2014). Regional correlation towards the south was following the established seismic-stratigraphy along the western Barents Sea margin (Faleide *et al.*, 1996; Jansen *et al.*, 1996).

Reflector R7 forms a group of low-amplitude discontinuous reflections near ODP Site 986, (Jansen *et al.*, 1996) (Fig. 6A-B; Table 2). On seismic profile A, reflector R7 defines the lower boundary of chaotic seismic facies near ODP Site 986 and southwards (Figs. 3A and 6B). These chaotic seismic facies have previously been recognized to characterize the interval above R7 on a regional scale along the north-western Barents Sea – south-western Svalbard margin (Fiedler & Faleide, 1996; Imbo *et al.*, 2003; Lee *et al.*, 2007) with its greatest areal extent south of Site 986 (Figs. 4A-B), adjacent to the Storfjorden Trough Mouth Fan (Figs. 5A-B) and at about 74°40´N (Hjelstuen *et al.*, 1996) (Figs. 5A, 5C). Near the Storfjorden Trough Mouth Fan depocentre, reflector R7 is defining the lower boundary of continuous, parallel seismic facies (Hjelstuen *et al.*, 1996) (Fig. 7A).

On the synthetic seismogram reflector R6 corresponds to a large trough (Jansen *et al.*, 1996) (Fig. 6A). R6 is defined by low- to moderate-amplitude discontinuous reflection near ODP Site 986 but there is a high-amplitude reflection immediately above it (Jansen *et al.*, 1996) (Figs. 6A-B; Table 2). Reflector R6 marks a very distinct change in seismic character at ODP Site 986, from the essentially chaotic seismic facies below, to the distinctly acoustically stratified signature above (Jansen *et al.*, 1996) (Figs. 6A-B). On the outer shelf and upper slope reflector R6 is locally seen as an erosional surface (Fig. 7A-B), it is also partly truncated by reflector R5 (Hjelstuen *et al.*, 1996).

Reflector R5 correspond to a strong pick on the synthetic seismogram (Jansen *et al.*, 1996) (Fig. 6A). On the seismic profile A at ODP Site 986 it is characterized by a moderate- to high-amplitude continuous reflection (Jansen *et al.*, 1996) (Fig. 6B). Reflection R5 is recognized as an important depositional sequence boundary along the entire Barents Sea-Svalbard margin (e.g. Faleide *et al.*, 1996), and it is a clear erosional unconformity on the outer shelf and upper slope within the Storfjorden TMF (Faleide *et al.*, 1996), and locally truncates the R7 reflector (Hjelstuen *et al.*, 1996) (Fig. 7A-B).

5. Results - seismic characterization of depositional sequence GI (2.7 – 1.5 Ma)

Depositional sequence GI has a maximum thickness of 1400 ms (twt) shelfward in the central part of the study area (Figs. 7A, 7C), and its thickness also increases towards the north in the distal part of the margin. The average sedimentation rate of GI sediments is ca. 95 cm/kyr. This estimate is based on a mean thickness of 950 meter (825 ms (twt) with interval velocity of between ca. 2.4 km/s and 2.2 km/s (Jansen *et al.*, 1996)), and assuming deposition of GI between 2.7 and 1.5 Ma following the age model of Knies et al. (2009) and Rebesco et al. (2014). Depositional sequence GI is distinguished through a series of seismic facies (Fig. 3) described and subsequently interpreted below.

5.1 Chaotic to transparent/reflection-free seismic facies

Description

The seismic-stratigraphic interval between reflectors R7 and R6 is mainly characterized by a reflection-free to chaotic seismic facies formed by discontinuous and discordant reflections of variable seismic amplitudes (Figs. 3A-B). This facies has its greatest areal extent south of Site 986, adjacent to the northern part of the Storfjorden TMF, and forms the basis for identifying a chaotic to reflection-free seismic facies unit 1 (or simply SFU1) (Figs. 4A-C and 5A-B). Similar facies are also widely recognized in the southern part of the study area at about 74°40´N, the Kveitola TMF. There, the facies can be grouped into four thick and aerially extensive chaotic to reflection-free seismic facies units 2 to 5 (SFU2-5) (Figs. 5A, C).

<u>Seismic facies unit 1 (SFU1)</u> is recognized along the lower slope and basin floor in the south-western Svalbard margin and partly along the most northern part of the Barents Sea margin (Figs. 4A-C and 5A-B). The upper boundary of SFU1 has an irregular character due to presence of numerous arcuate-like ridges of various dimensions (Fig. 4D). The lower boundary of SFU1 is well defined by a high amplitude continuous reflection, which is parallel to the underlying undisturbed and well-stratified strata formed by plane-parallel high-amplitude reflections (Fig. 4D). The lower boundary of SFU1 often coincide with the reflector R7 in the basinward direction (Figs. 4A-C and 5A-B).

SFU1 extends at least 250 km along the margin, has a length (measured from west to east) of at least 140 km and its mapped areal extent covers 10.7×10^3 km^2 (Fig. 2A). It is thinning towards the south (Fig. 2B), but its exact termination is fairly unclear as a chaotic seismic signature gradually becomes stratified (Figs. 5A-B). SFU1 pinches out both towards the basin floor further to the west and the continental slope to the east (Fig. 2B), where it locally terminates towards an erosional semi-circular scar-like feature (Figs. 8A-B) which is ca. 140 ms (twt) height. SFU1 shows a general trend of increasing thickness in the downslope direction (Fig. 2B). A maximum mapped thickness of SFU1 is ca. 870 m (not decompacted) or 0.720 s (twt) considering an average interval velocity of 2.40 km/s within the seismic interval between reflectors R7 and R6 (Jansen *et al.*, 1996). The "minimum" estimated volume of the mapped deposits involved is more than 4.1×10^3 km^3assuming a mean thickness of 0.317 s (twt) or ca. 380 m. However, SFU1 likely has much larger areal extent of at least 19.4×10^3 km^2, because it can potentially be traced further to the north and west outside the mapped area based on its time-thickness map (Fig. 2B). Therefore, a "maximum" estimated volume of deposits involved in this interval is probably about 7.4×10^3 km^3assuming a mean thickness of at least 380 m.

Sample analysis from the ODP Site 986 through the chaotic seismic facies unit 1 showed that it is mainly formed by sand and silty clay, and interpreted as debris flow deposits interbeded with hemipelagic sediments (Forsberg *et al.*, 1999; Butt *et al.*, 2000). Sandy debris flow deposits precluding turbidites due to lack of normal grading and traction features, and high smectite content, which provides the sediment thixotropic properties conducive to movement as a cohesive debris flow (Forsberg et al., 1999; Butt et al., 2000).

Seismic facies units 2-5 (SFU2-SFU5) are recognized along the lower slope and basin floor southwards from SFU1, in the north-western part of the Barents Sea margin covered by the Kveitola TMF (Figs. 5A and 9A-B). SFU2-5 are lens-shaped in cross-section and are characterized by a chaotic to partly reflection-free seismic pattern similar to previously described SFU1 (Figs. 5C and 9C). However, the internal seismic pattern also includes localized subparallel, steeply dipping reflections partly affecting the relief of the top surface by forming ridges (Fig. 9C). SFU2-SFU5 do not show any indication of erosion and are separated by single well-defined continuous reflectors, mainly restricted to the deepest part of the study area (lower slope and basin floor) (Figs. 5A, 5C) and by sets of well-defined continuous reflectors at their proximal position (in the upper slope) (Fig. 9C). The maximum total thickness of these four chaotic to reflection-free seismic facies units within the mapped area is ca. 750 ms (twt) or ca. 900 m considering an average interval velocity of 2.40 km/s within the seismic interval between reflectors R7 and R6 (Jansen *et al.*, 1996). SFU2-5 pinch out gradually towards the east to the upper slope, thinning towards the far distal part of the basin floor (Fig. 9B), and thinning southwards and northwards (Fig. 5A). Scar-like features similar to that in the north of the study area are not observed within the depositional sequence GI in the south, potentially due to poor seismic resolution. However, a slightly curved high amplitude feature in the upper slope may be a potential palaeo-scar (Fig. 9D).

Seismic facies units 2, 3, 4 and 5 are similar to each other in terms of their areal extent and thickness. The characteristics of all four units can be summarized using seismic facies unit 3 (SFU3) as an example. SFU3 extends at least 110 km along the margin and has a length (measured from west to east) of at least 130 km (Fig. 2A). It has an areal extent of at least 7.04×10^3 km^2 of SU3. Its time-thickness map suggests thickening towards the basin floor up to 245 ms (twt) or 294 m assuming an average interval velocity of 2.40 km/s (Fig. 2C). The "minimum" volume of sediments within SFU3 is more than 1.1×10^3 km^3 taking into account a mean thickness of 150 m (125 ms (twt)) and interval velocity of 2.40 km/s within the study interval. However, the "maximum" estimated volume is about $1,5\times10^3$ km^3 considering a larger area of at least 9.8×10^3 km^2 (based on the time-thickness map of SFU3 and regional seismic profile indicating SFU3 eastern continuation further to the east) and the same mean thickness of at least 150 m (Fig. 2 C).

Interpretation

The chaotic to reflection-free seismic facies within the stratigraphic interval between the reflectors R6 and R7 has earlier been inferred to be mass movement deposits (Faleide *et al.*, 1996; Hjelstuen *et al.*, 1996). Our study has shown that these facies are more complex and include: (1) a massive and regionally extensive seismic facies unit 1 (SFU1) in the north of the study area (Figs. 4B and 5A) and (2) a set of several seismic facies units (SFU2-SFU5) in the south (Figs. 5A and 9B). A smooth, low-relief base of the five seismic facies units, seen as a continuous and high-amplitude reflection parallel to the underlying strata, indicate that the mass movements occurred along a plane of weakness, and one particular stratigraphic level acted as a glide plane. Mass movements bounded by distinct failure planes following the stratification of the underlying strata have been identified in several studies including the Storegga Slide (Bugge *et al.*, 1987) and the Trænadjupet Slide (Lindberg *et al.*, 2004). A slide origin is also supported by the termination of SFU1 towards a palaeo-scar (Fig. 8B) suggesting that it is a translational slide deposit according to the definition of Lee et al. (2007), and that this scar represents a headwall similar to those associated with Bjørnøya Fan Slide III (Hjelstuen *et al.*, 2007) and the Storegga Slide complex (Solheim *et al.*, 2005).

The chaotic seismic expression of SFU1-5 is an indication of a high degree of stratum disturbance, which is interpreted here to be a result of the transition from submarine slide to various mass flows such as debris flows and/or turbidity currents (e.g. Laberg & Vorren, 1993; Mulder & Cochonat, 1996; Lee *et al.*, 2007). Similar facies are typical for debris flow deposits described elsewhere, for example, within the Pleistocene Bjørnøya Fan Slide Complex, SW Barents Sea margin (Hjelstuen *et al.*, 2007) and the Gebra submarine slide, Antarctica (Imbo *et al.*, 2003). Sample analysis from the ODP Site 986 through this interval showed that these facies are mainly formed by sand and silty clay, and interpreted as debris flow deposits interbeded with hemipelagic sediments (Forsberg *et al.*, 1999; Butt *et al.*, 2000). The reflection-free parts are likely to be interpreted as thick seismically homogeneous sandstones or shale (Mitchum *et al.*, 1977). Therefore, it is interpreted that once the slide mass started to move, it probably rapidly disintegrated and transformed into a debris flow, which may occur over a distance of only a few kilometers (Morgenstern, 1967; Hampton, 1972; Laberg & Vorren, 2000; Lee et al., 2007). The chaotic to reflection-free seismic facies units 1-5 are therefore referred to during this study as slide debrites 1-5.

The presence of at least four large-scale slide debrites (SFU2-SFU5) in the south of the study area suggests repeated failures in this area. The presence of continuous high-amplitude reflections in between each of the slide debrites is interpreted to indicate a period of hemipelagic and/or glacio-marine(?) deposition, analogous with the Bjørnøya Fan Slide Complex (Hjelstuen *et al.*, 2007).

The ridges observed along the top surface of the slide debrites SFU2-SFU5 (Figs. 4D and 9C) are interpreted here as pressure ridges developing perpendicular to the main flow direction to which the maximum compressive stress is oriented (Laberg *et al.*, 2001; Dahlgren *et al.*, 2005). This interpretation is also supported by the presence of steeply dipping parallel reflections separated by offsets within the submarine slide debrites SFU2-SFU5, which are similar to small-scale thrusts forming the pressure ridges in the top surface of a submarine mass-transport complex from offshore Norway (Mosar *et al.*, 2002) (Fig. 9C). Pressure ridges have usually been reported to be associated with debris flow deposits (Eiken & Hinz, 1993), and they usually occur where mass-transport complexes are free to spread out across the seafloor in an unconfined manner (Prior *et al.*, 1984; Mosar *et al.*, 2002; Dahlgren *et al.*, 2005; Amundsen *et al.*, 2011). For comparison, frontally confined mass-transport complexes are usually characterized by the development of large-scale fold and thrust systems (e.g. Faugeres *et al.*, 1999; Mosar *et al.*, 2002; Dahlgren *et al.*, 2005), which are not observed during this study.

5.2 Parallel - subparallel seismic facies

Description

The seismic-stratigraphic interval between reflectors R7 and R6 on the upper slope of the study area is mainly characterized by continuous, parallel to subparallel, medium- to high-amplitude seismic reflections (Figs. 3C-D and 7A). Rather continuous, parallel to sub-parallel, low- to medium-amplitude seismic reflections are also recognized in the lower slope near the Storfjorden TMF depocentre (Figs. 5A and 7A). They are delineated by the chaotic to reflection-free seismic facies unit SFU1 from the north and SFU2-5 from the south (Fig. 5A).

Within the study area the seismic-stratigraphic interval between the reflectors R6 and R5 is generally characterized by continuous, parallel and sub-parallel, medium-to high-amplitude seismic reflections (Figs. 5A, 7A and 9A-B). The interval is thickening towards the slope. Sample analysis from the ODP Site 986 through these facies showed that they are characterized by an increase in clay content up to ca. 30%, decrease in a total fine sand content to between 5% and 20% and an increase in the amount of particles of more than 0.5 mm in size (Forsberg *et al.*, 1999; Butt *et al.*, 2000). These facies were interpreted to be formed by stacked glacigenic debris flows deposits and turbdites interbedded with hemipelagic sediments (Jansen *et al.,* 1996; Butt *et al.,* 2000).

In the north-west a steep-dipping scar-like feature is infilled by seismic facies formed by continuous, parallel, medium- to high-amplitude seismic reflections (Figs. 8A-B). These reflections are onlapping onto the scar and revealing a progressive upslope accretion within the scar (Fig. 8B). These facies are also parallel with the upper boundary of the chaotic to reflection-free seismic facies unit 1.

Interpretation

Well-stratified seismic facies within the depositional sequence GI are interpreted here as marine hemipelagic sediments based on similarities with seismic facies from the late Pliocene-Pleistocene sediments along the western Barents Sea margin (Hjelstuen *et al.*, 1996; Dahlgren *et al.*, 2005; Hjelstuen *et al.*, 2007). Similar seismic facies can be also interpreted as partly glacimarine sediments predomenantly deposited from meltwater overflows and underflows (Dahlgren *et al.*, 2005). It can in particularly be applicable to the seismic-stratigraphic interval between the reflectors R6 and R5 characterized by presence of fractions more than 0.5 mm including both IRD and clasts that suggests their glacial origin (Butt *et al.,* 2000). Abundant dropstones are also present within this interval (Jansen *et al.,* 1996).

Continuous, parallel, medium- to high-amplitude seismic reflections within the palaeo-scar recognized in the depositional sequence GI on the continental slope (Figs. 8A-B) are interpreted as infilling contouritic drift similar to the Late Cenozoic infilling Sklinnadjupet Drift in the northern Norwegian Sea (Laberg *et al.*, 2001).

5.3 Contorted seismic facies

Description

In the far north of the study area, along the SW Svalbard margin, the stratigraphic interval between the reflectors R6 and R5 is partly characterized by contorted seismic facies formed by relatively continuous, high-amplitude reflections (Figs. 3E and 4C). It is not possible to map this unit in three dimension due to lack of 2D seismic data crossing this facies.

Interpretation

Contorted seismic facies within the seismic-stratigraphic interval between the reflectors R6 and R5 are typical for contouritic deposits (Faugeres *et al.*, 1999; Rebesco & Stow, 2001) (Fig. 4C). The presence of contouritic sediments have also been suggested within the Pliocene-Pleistocene succession north of the study area (Eiken & Hinz, 1993) and, in particular, within the same stratigraphic interval along the SW of Svalbard - Bellsund TMF (Amundsen *et al.*, 2011) (Fig. 1A).

6. Discussion

6.1. The failed sediments: timing, size and source area

Published literature has documented the importance of large-scale submarine sliding for transporting large volumes of sediments into the deep-water basins (e.g. Lee *et al.,* 2007). Along the Norwegian – Barents Sea – Svalbard continental margin, such events have mainly been inferred to be younger than 1.0 Ma and closely related to large scale intensification of glaciation in the Northern Hemisphere (e.g. Elverhøi *et al.*, 2002). Formation of large-scale debris flow deposits was, in particularly, associated with episodes when an ice sheet was reaching the shelf break (Laberg *et al.*, 2010) (Fig. 10, Table 1). Subglacial deformation till was in this case deposited on the outer shelf and uppermost slope, and subsequently remobilized to form glacigenic debris flows (Laberg *et al.*, 2010).

This study finds that large-scale submarine slide debrites 1-5, recognized in the stratigraphic interval between reflectors R7 and R6, were formed during the time period from 2.7 to 2.1 Ma (following the revised age model of Rebesco et al. (2014) (Fig. 10; Table 2). This time corresponds to an initial glacial growth phase in the Northern Hemisphere (Knies *et al.*, 2009). During this time the glaciers most likely did not reach the shelf edge in the study area and terminated on land (Jansen *et al.,* 2000; Butt *et al.,* 2002; Knies *et al.,* 2009). A new correlation of seismic data to the ODP Site 986 suggests that it is reflector R4A (~1.3 Ma) (Table 2) that marks the onset of Storfjorden TMF growth (Rebesco *et al.*, 2014), and hence the onset of shelf-edge glacial development along the NW Barents Sea margin. Seismic data along the southwestern Barents Sea margin indicate the presence of ice sheets extending to the shelf break only since ~ 1.5 Ma (seismic reflector R5) (Andreassen *et al.,* 2004).

Sedimentological data from the ODP Site 986 also indicated that the study area was apparently free of any major ice sheets during the time period of the slide debrites 1-5 formation. The ice sheet was reaching the shelf edge later, from the time of reflector R6 and onwards (Forsberg *et al.*, 1999; Butt *et al.*, 2000). The stratigraphic interval between the reflectors R7 and R6 is formed by silty clay and characterized by dramatic increase in fine sand content from approximately 2-3% to 20-40% (Jansen *et al.*, 1996). This interval is characterized by very limited amount of grains coarser than 0.5 mm, which include glass shards and elongated pellets appearing to be infilled of fossil burrows (Butt *et al.*, 2000). Therefore, these particles have been interpreted not to be classified as true ice rafted detritus (IRD) and not be related to drifting or calving ice (Butt *et al.*, 2000).

To summarize, formation of large-scale slide debrites 1-5 most likely took place before the shelf-edge glaciation in the study area when the glaciers were terminating on land (Fig. 10). Fluvial and glaciofluvial drainage probably acted as the main sediment transport mechanisms into the marine realm, and downslope transport was as sliding/slumping, debris flows, and turbidity currents (Forsberg *et al.*, 1999; Butt *et al.*, 2000). Mineralogical analysis of the sediments at Site 986, indicating very low carbonate content and high smectite content among the clays (Forsberg *et al.*, 1999; Butt *et al.*, 2000), together with the paleontological evidence (Smelror, 1999), suggested that a subaerially exposed Barents Sea acted as the principle source of sediments below the reflector R6.

Table 1 shows that the submarine slide debrites 1-5 are comparable and sometimes even larger in terms of volume than submarine slides along the NE Atlantic margin formed during the shelf-edge glaciation. For example, the submarine slide debrite 1 remobilized at least one and a half times more sediments than one of the largest exposed submarine slides in the world – the Storegga Slide in the Norwegian Sea. The total volume of remobilized sediments by the slide debrites 1-5 is more than 9.6×10^3 km^3. It is approximately one quarter of the total volume of sediments deposited during the time GI (2.7-1.5Ma) along the NW Barents Sea (Hjelstuen *et al.*, 1996). It is also approximately four times less than the total volume of sediments transferred to the deep sea due to sediments failure over the last ~1.5Ma along the NW Barents Sea margin. Thus, submarine sliding played an important role in the deep-water sediment evolution along the NW Barents Sea margin during the time period between 2.7 and

2.1 Ma before the shelf-edge glaciation. A similar conclusion was also reached by Hjelstuen and Andreassen (2015) studying the southernmost part of the Norwegian continental margin. They reported the presence of a giant Norway Basin Slide A (NBS-A), which covers an area of 63,700 km^2, containing a sediment volume of 24,600 km^3, and which reaches a maximum thickness of ca. 650m. This failure also formed before the first ice sheet advanced to the Norwegian margin shelf edge.

6.2 Factors promoting failure of the NW Barents Sea margin and deposition of slide debrites 1-5

Submarine slides occur as a result of either a decrease in the resisting/shear strength of the continental slope sediments, an increase in the downward-oriented driving/shear stresses (environmental loads), or a combination of the two factors (Laberg & Vorren, 2000; Lee *et al.*, 2007). There are several preconditioning factors and final triggering mechanisms that can be of importance for promoting sliding in the study area. Preconditioning factors include (1) low eustatic sea-level, (2) high sedimentation rate, (3) the presence of regionally extensive weak layer(s), (4) presence of gas and/or gas hydrates (e.g. Knutsen *et al.*, 1993; Laberg & Vorren, 2000; Imbo *et al.*, 2003; Lindberg *et al.*, 2004; Evans *et al.*, 2005). A combination of factors often leads to failure (Imbo *et al.*, 2003) as will be further discussed. The triggering mechanism is an external stimulus that initiates the slope instability (Sultan *et al.*, 2004).

6.2.1 Preconditioning factors

─ *Low eustatic sea level* is one of the major mechanisms for debris flows and mega turbidites formation in a deep-water environment at non-glaciated margins (e.g. Leynaud *et al.,* 2009) by erosion or bypass of the shelf and subsequent direct sediment transport into the deep-water environment by gravity flows (e.g. Emery & Myers, 1996). The frequency of mega events is also higher on non-glaciated margins, but the total volume of mobilized sediments from mass wasting is much larger on the glaciated margin (Maslyn *et al.,* 2004). Cenozoic eustatic-cycle chart do in fact shows a global eustatic sea-level falling initiated during the late Pliocene time and continued falling during the early Pleistocene (Vail *et al.*, 1977; Veeken & Moerkerken, 2013). Therefore, prior to the presence of the ice sheet at the shelf break an eustatic low sea level may have acted as a preconditioning factor for the formation of large scale submarine slide debrites 1-5 within the study area. Unfortunately, it is not possible to provide a reliable correlation between late Pliocene-early Pleistocene episodes of gradual global eustatic sea-level fallings with sea-level changes in the study area due to lack of high-resolution biostratigraphic data from the interval of interest. In addition, the regional sea-level variation of the study area may not simply mirror the global eustatic trend as the periodic presence of an ice sheet on the shelf may introduce isostatic effects amplifying or reducing eustatic variations in sea-level. Therefore, the effect of this mechanism may be less on glaciated continental margins as compared to non-glaciated margins.

— ***Rapid sedimentation*** can lead to build-up of excess pore pressure and under-consolidation of sediments and consequently shear strength reduction (Laberg & Vorren, 2000; Lindberg *et al.*, 2004). The average sedimentation rate during deposition of depositional sequence GI sediments is calculated to ca. 72 cm/ka from a mean thickness of ca. 750 ms (860 m; not decompacted) and an interval velocity for GI of ~2.3 km/s (Jansen *et al.,* 1996). These rates are markedly higher than the estimated rates for the corresponding period in the SW Barents Sea (Hjelstuen *et al.*, 2007), and (2) comparable with the rates for the succeeding ~1.5-1.0 Ma period of the SW Barents Sea margin (Hjelstuen *et al.*, 2007), during which the ice sheet repeatedly reached the shelf break Andreassen *et al.* (2007). Thus, we suggest that the sedimentation rate during time GI was relatively high and potentially could have been sufficient to build-up an excess in pore pressure within the studied deposits. This is in conformity with Butt et al. (2000) who suggested that a subaerially exposed Barents Sea with increased moisture transport accounted for high sedimentation rates, which caused rapid build-up of sediments at the shelf break and led to downslope movement of sediments as debris flows.

— ***Presence of regionally extensive weak layers*** may have influenced the continental slope stability (Laberg & Vorren, 2000; Lindberg *et al.*, 2004), and it can be considered as another potential preconditioning factor for sediments failure presented during this study. The studied submarine slide debrites are defined by prominent high-amplitude basal seismic reflections parallel to the underlying undisturbed strata. This likely indicates that sliding occurred along one particular stratigraphic horizon or weak layer, which had lower shear strength than older and younger sediments. A glide plane could have developed within contouritic sediments. For both large-scale submarine slides (the Storegga Slide (Bryn et al., 2003); the Nyk Slide (Lindberg *et al.*, 2004); the Trænadjupet Slide (Laberg *et al.*, 2003) and smaller-scale slides (e.g. Beaten *et al.*, 2013), contouritic sediments have been reported to be the sediments that initially failed as they have higher water content and lower density than the overlying sediments indicating low shearing resistance with these sediments (Laberg *et al.*, 2003). The presence of contouritic sediments have been indicated within the seismic-stratigraphic interval between reflectors R6 and R5 along the south-western Svalbard margin (Fig. 4C) and the north-western Barents Sea margin (Fig. 8B). These contourites are however younger than the submarine slide debrites 1-5. Slightly contorted nature of the continuous high-amplitude reflections in the seismic-stratigraphic interval between reflectors R7 and R6 and in the interval below reflector R7 may be potentially interpreted as due to the presence of contourites (Fig. 4C). This interpretation can be supported by previous studies, which suggested the presence of contouritic sediments within the pre-glaciogenic late Miocene-Pliocene and late Pliocene-Pleistocene predominantly glaciogenic sediments in the west of Svalbard (Eiken & Hinz, 1993; Amundsen *et al.,* 2011). The onset of contouritic current in the western Svalbard margin has been suggested to be related to opening of the gateway between Svalbard and Greenland, Late Cenozoic climate cooling, or to paleographic changes (Laberg *et al.,* 2005).

– ***Presence of gas and gas hydrates*** in sediments can cause sliding (e.g. Knutsen *et al.*, 1993) because gas charging can decrease the sediment strength through development of excess pore pressure (Lee *et al.*, 2007). A change in the pressure and/or bottom water temperature can cause a release of large amounts of free gas from decomposed gas hydrates and decrease the shear strength along stratigraphic layers (Bugge *et al.*, 1987; Lindberg *et al.*, 2004). The presence of gas and a zone of methane hydrates (between 20 and 150 m below sea-level) were indicated in the ODP Site 986 showing that gas hydrates are stable in this deep-sea setting during the present day conditions, but it is not known whether gas hydrates were stable during the time period between 2.7 and 1.5 Ma (Jansen *et al.*, 1996). Due to lack of direct evidences, presence of gas and gas hydrates is considered to be a less likely preconditioning factor in order to generate large-scale submarine sliding in the study area.

6.2.2 Triggering mechanism

The most likely mechanism for triggering large scale sliding in the study area is considered to be the occurrence of one or more earthquakes. Submarine slides triggered by earthquakes have been reported worldwide, including Norwegian-Barents Sea margin (e.g. Bugge *et al.*, 1987; Laberg & Vorren, 1993; 2000). Earthquakes have also been suggested as a major triggering mechanism for the non-glaciated low-latitude margins (south of 52°N) (e.g. Leynaud *et al.,* 2009). Firstly, it can be explained by the ability of earthquake shaking, in a submarine setting, to produce quite large shear stresses relative to shear strength and thus cause sediment failure (Lee *et al.*, 2007). Secondly, earthquake-induced shear stresses can contribute to the ambient gravitational stresses and cause a previously stable slope to deform and fail. Thirdly, earthquake-induced cyclic stresses can also generate excess pore-water pressure, which can decrease the shear strength even more and lead to liquefaction of sediments. Frequent lower magnitude earthquakes in comparison with a large magnitude event has been considered a likely triggering of a large-scale slope failure elsewhere (Mosher *et al.*, 1994).

The studied slide debrites 1-5 are closely associated with major tectonic lineaments within the Spitsbergen Shear Zone (Fig. 2A) suggesting their influence on a failure. Large number of earthquakes of magnitude ≤ 6 have been detected since 1750 within the Spitsbergen Shear Zone, to a large degree associated with tectonic lineaments (e.g. the Hornsund Fault Zone (74°30'-81°N)) and Knipovich and Mohns rifts valleys (Avetisov, 1996; Crane *et al.*, 2001).

During this study we suggest that earthquakes could potentially took place during the time of the slide debrites 1-5 formation tacking into account that Knipovich Ridge and the Hornsund Fault Zone were already active at that time. Formation of the Knipovich Ridge and the Hornsund Fault Zone took place as the result of opening of the Norwegian-Greenland Sea initiated in the early Eocene (e.g. Faleide *et al*., 2008). The change in plate configuration and spreading direction in the earliest Oligocene resulted in a northward opening of the Greenland Sea between Greenland and Svalbard, first by continent extension, followed by incipient sea-floor spreading along the Knipovich Ridge (Lundin & Dore, 2002; Mosar *et al*., 2002). Since the Mid-Oligocene the Hornsund Lineament is supposed to have been the active fault system between Svalbard and Greenland (Eldholm *et al.*, 1987; Eiken, 1993).

To summarize, the preconditioning factors for submarine sliding in this area probably included deposition at high sedimentation rate, some of which possibly occurred in periods of low stand of sea-level. Intervals of weak contouritic sediments might also have contributed to the instability of part of the slope succession (Fig. 11). Failures were likely triggered by earthquakes due to the location of the slides close to seismically active spreading axes and tectonic lineaments at the time of formation.

7. Conclusions

1. The NW Barents Sea passive continental margin reveals the existence of large-scale submarine slide debrites formed between 2.7-2.1 Ma, most likely, before shelf-edge glaciation.
2. The largest of them, submarine slide debrite 1 is located in the north of the study area and associated with a palaeo-scar. It has a maximum thickness of ca. 866 m, covers an area of more than 10.7×10^3 km^2 and contains over 4.1×10^3 km^3 of sediments, more than the biggest “modern” slide, the Storegga Slide on the mid Norwegian margin.
3. South in the study area, at least four large-scale slide debrites were identified, all smaller than the submarine slide debrite 1. Each of them is ca. 295 m thick, covers an area of at least 7.04×10^3 km^2 and involved $1{,}1\times10^3$ km^{3}of sediments. These submarine slide debrites lack clearly defined scars.
4. Low eustatic sea-level in combination with high sedimentation rates with some potential presence of weak layers - contourites are suggested as most likely preconditioning factors for sliding in the study area. Earthquakes, associated with the Knipovich spreading ridge and tectonic activity along old lineaments within the Spitsbergen Shear Zone, are final triggering mechanism of the slope failures in the study area.

Acknowledgments

This work was carried out as part of a PhD research and is a contribution to the Petromax project “Depositional models for Cenozoic sandy systems (Democen)” financially supported by the Norwegian Research Council (NFR), Statoil and the University of Tromsø. The study is also a contribution to “Centre for Arctic Gas Hydrate, Environment and Climate (CAGE)” (NFR grant 200672) and the ARCEx project (Research Centre for Arctic Petroleum Exploration) which is funded by the Research Council of Norway (grant number 228107) together with 10 academic and 9 industry partners. The authors are thankful to the Russian Joint Stock Company “Russian Marine Arctic Geological Expedition” (MAGE) for providing seismic data. We would like to thank J.P. Holm who produced an introduction figure and S.

Polyanov who helped with geophysical data. We offer our sincere thanksto J. Duncan for correcting the English language. The manuscript benefited from constructive and helpful reviews by L. Moscardelli, B. Reece and C. Jackson.

Conflict of Interest

No conflict of interest declared.

References

AMUNDSEN, I.M., BLINOVA, M., HJELSTUEN, B.O., MJELDE, R. & HAFLIDASON, H. (2011) The Cenozoic Western Svalbard Margin: Sediment Geometry and Sedimentary Processes in an Area of Ultraslow Oceanic Spreading. *Marine Geophysical Researches*, **32,** 441-453.

ANDREASSEN, K., NILSSEN, E.G. & ODEGAARD, C.M. (2007) Analysis of Shallow Gas and Fluid Migration within the Plio-Pleistocene Sedimentary Succession of the Sw Barents Sea Continental Margin Using 3d Seismic Data. *Geo-Marine Letters*, **27,** 155-171.

AVETISOV, G.P. (1996) *Seismically Active Zones of the Arctic*. Saint Petersburg VNIIOkeangeologia.

BEATEN, N., J,, LABERG, J.S., FORWICK, M., VORREN, T.O., VANNESTE, M., FORSBERG, C.F., KVALSTAD, T.J. & IVANOV, M. (2013) Morphology and Origin of Smaller-Scale Mass Movements on the Continental Slope Off Northern Norway. *Geomorphology*, **187,** 122-134.

BROWN, A.R. (1999) *Interpretation of Three-Dimensional Seismic Data*. SEG Investigations in Geophysics.

BUGGE, T. (1983) *Submarine Slides on the Norwegian Continental Margin, with Special Emphasis on the Storegga Area*. Continental Shelf and Petroleum Research Institute Publication, Trondheim, Norway.

BUGGE, T., BEFRING, S., BELDERSON, R.H., EIDVIN, T., JANSEN, E., KENYON, N., HOLTEDAHL, H. & SEJRUP, H.P. (1987) A Giant Three-Stage Submarine Slide Off Norway. *Geo-Marine Letters*, **7,** 191-198.

BUTT, F.A., ELVERHøI, A., SOLHEIM, A. & FORSBERG, C.F. (2000) Deciphering Late Cenozoic Development of the Western Svalbard Margin from Odp Site 986 Results. *Marine Geology*, **169,** 373-390.

CANALS, M., LASTRAS, G., URGELES, R., CASAMOR, J.L., MIENERT, J., CATTANEO, A., BATIST, M.D., HAFLIDASON, H., IMBO, Y., LABERG, J.S., LOCAT, J., LONG, D., LONGVA, O., MASSON, D.G., SULTAN, N., TRINCARDI, F. & BRYAN, P. (2004) Slope Failure Dynamics and Impacts from Seafloor and Shallow Sub-Seafloor Geophysical Data: Case Studies from the Costa Project. *Marine Geology*, **213,** 9-72.

CRANE, K., DOSS, H., VOGT, P., SUNDVOR, E., CHERKASHOV, G., POROSHINA, I. & JOSEPH, D. (2001) The Role of the Spitsbergen Shear Zone in Determining Morphology, Segmentation and Evolution of the Knipovich Ridge. *Marine Geophysical Researches*, **22,** 153-205.

DAHLGREN, K.I.T., VORREN, T., STOKER, M.S., NIELSEN, T., NYGåRD, A. & SEJRUP, H.P. (2005) Late Cenozoic Prograding Wedges on the Nw European Continental Margin: Their Formation and Relationship to Tectonics and Climate. *Marine and Petroleum Geology*, **22,** 1089-1110.

DOWDESWELL, J.A. & COFAIGH, O. (2002) *Glacier-Influenced Sedimentation on High-Latitude Continental Margins*. Geological Society, Special Publication, London.

EIDVIN, T., JANSEN, E. & RIIS, F. (1993) Chronology of Tertiary Fan Deposits Off Western Barents Sea: Implications for the Uplift and Erosion History of the Barents Sea Shelf. *Marine Geology*, **112,** 109-131.

EIDVIN, T., GOLL, R.M., GROGAN, P., SMELROR, M. & ULLEBERG, K. (1998) The Pleistocene to Middle Eocene Stratigraphy and Geological Evolution of the Western Barents Sea Continental Margin at Well Site 7316/5-1 (Bjørnøya West Area). *Norwegian Journal of Geology*, **78,** 99-123.

EIDVIN, T., JANSEN, E., RUNDBERG, Y., BREKKE, H. & GROGAN, P. (2000) The Upper Cainozoic of the Norwegian Continental Shelf Correlated with the Deep Sea Record of the Norwegian Sea and the North Atlantic. *Marine and Petroleum Geology*, **17,** 579-600.

EIKEN, O. (1993) An Outline of the Northwestern Svalbard Continenal Margin. In: *Arctic Petroleum Potential* (Ed. by T. O. Vorren, E. Bergsager, Ø. A. Dahl-Stamnes, E. Holter, B. Johansen, E. Lie & T. B. Lund), **2**, 619-629. NPF Special Publication, Elsevier, Amsterdam.

EIKEN, O. & HINZ, K. (1993) Contourites in the Fram Strait. *Sedimentary Geology*, **82,** 15-32.

ELDHOLM, O., FALEIDE, J.I. & MYHRE, A.M. (1987) Continent-Ocean Transition at the Western Barents Sea/Svalbard Continental Margin. *Geology*, **15,** 1118-1122.

ELVERHøI, A., BLASIO, F.V., BUTT, F.A., ISSLER, D., HARBITZ, C., ENGVIK, L., SOLHEIM, A. & MARR, J. (2002) Submarine Mass-Wasting on Glacially-Influenced Continental Slopes: Processes and Dynamics. In: *Glacier-Influenced Sedimentation on High-Latitude Continental Margins* (Ed. by D. J.A. & O. Cofaigh), 73-87. Geological Society, London, Special Publications.

EMERY, D. & MYERS, K.J. (1996) *Sequence Stratigraphy*. Blackwell, Oxford.

EVANS, D., HARRISON, Z., SHANNON, P.M., LABERG, J.S., NIELSEN, T., AYERS, S., HOLMES, R., HOULT, R.J., LINDBERG, B., HAFLIDASON, H., LONG, D., KUIJPERS, A., ANDERSEN, E.S. & BRYN, P. (2005) Palaeoslides and Other Mass Failures of Pliocene to Pleistocene Age Along the Atlantic Continental Margin of Nw Europe. *Marine and Petroleum Geology*, **22,** 1131-1148.

FALEIDE, J.I., SOLHEIM, A., FIEDLER, A., HJELSTUEN, B.O., ANDERSEN, E.S. & VANNESTE, K. (1996) Late Cenozoic Evolution of the Western Barents Sea-Svalbard Continental Margin. *Global and Planetary Change*, **12,** 53-74.

FAUGERES, J.-C., STOW, D.A.V., IMBERT, P. & VIANA, A. (1999) Seismic Features Diagnostic of Contourite Drifts. *Marine Geology*, **162,** 1-38.

FIEDLER, A. & FALEIDE, J.I. (1996) Cenozoic Sediemntation Along the Southwestern Barents Sea Margin in Relation to Uplift and Erosion of the Shelf. *Global and Planetary Change*, **12,** 75-93.

FORSBERG, C.F., SOLHEIM, A., ELVERHOI, A., JANSEN, E., CHANNELL, J.E.T. & ANDERSEN, E.S., eds. (1999) *The Depositional Environment of the Western Svalbard Margin During the Late Pliocene and the Pleistocene: Sedimentary Facies Changes at Site 986.* Proceeding Ocean Drilling Program. Scientific Results. Ocean Drilling Program, College Station, TX.

HAFLIDASON, H., SEJRUP, H.P., NYGåRD, A., MIENERT, J., BRYAN, P., LIEN, R., FORSBERG, C.F., BERG, K. & MASSON, D. (2004) The Storegga Slide: Architecture, Geometry and Slide Development. *Marine Geology*, **213,** 201-234.

HJELSTUEN, B.O., ELVERHøI, A. & FALEIDE, J.I. (1996) Cenozoic Erosion and Sediment Yield in the Drainage Area of the Storfjorden Fan. *Global and Planetary Change*, **12,** 95-117.

HJELSTUEN, B.O., ELDHOLM, O. & FALEIDE, J.I. (2007) Recurrent Pleistocene Mega-Failures on the Sw Barents Sea Margin. *Earth and Planetary Science Letters***,** 605-618.

HJELSTUEN, B.O. & ANDREASSEN, E.V. (2015) North Atlantic Ocean Deep-Water Processes and Depositional Environments: A Study of the Cenozoic Norway Basin. *Marine and Petroleum Geology*, **59,** 429-441.

IMBO, Y., BATIST, M.D., CANALS, M., PIETO, M.J. & BARAZA, J. (2003) The Gebra Slide: A Submarine Slide on the Trinity Peninsula Margin, Antarctica. *Marine Geology*, **193,** 235-252.

JANSEN, E., RAYMO, M.E. & BLUM, P. (1996) Site 986. *Proceeding of the Ocean Drilling Program, Initial Reports*, **162,** 287-343.

KNIES, J., MATTHIESSEN, J., VOGT, C., LABERG, J.S., HJELSTUEN, B.O., SMELROR, M., LARSEN, E., ANDREASSEN, K., EIDVIN, T. & VORREN, T.O. (2009) The Plio-Pleistocene Glaciation of the Barents Sea–Svalbard Region: A New Model Based on Revised Chronostratigraphy. *Quaternary Science Reviews.*, **28,** 812-829.

KNUTSEN, S.M., RICHARDSEN, G. & VORREN, T. (1992) Late Miocene-Pleistocene Sequence Stratigraphy and Mass-Movements on the Western Barents Sea Margin. In: *Arctic Geology and Petroleum Potential* (Ed. by T. Vorren, E. Bergsager, Ø. A. Dahl-Stamnes, E. Holter, B. Johansen, E. Lie & T. B. Lund), 573-606. Norwegian Petroleum Society Special Publication N. 2, Elsevier, Amsterdam.

KNUTSEN, S.M., RICHARDSEN, G. & VORREN, T.O. (1993) Late Miocene-Pleistocene Sequence Stratigraphy and Mass-Movements on the Western Barents Sea Margin. In: *Arctic Geology and Petroleum Potential* (Ed. by T. O. Vorren, E. Bergsager, Ø. A. Dahl-Stamnes, E. Holter, B. Johansen, E. Lie & T. B. Lund), 573-606. Norwegian Petroleum Society Amsterdam.

KUVAAS, B. & KRISTOFFERSEN, Y. (1996) Mass Movements in Glaciomarine Sediements on the Barents Sea Continental Slope. *Global and Planetary Change*, **12,** 287-307.

LABERG, J.S. & VORREN, T.O. (1993) A Late Pleistocene Submarine Slide on the Bear Island Trough Mouth Fan. *Geo-Marine Letters*, **13,** 227-234.

LABERG, J.S. & VORREN, T.O. (1996) The Middle and Late Pleistocene Evolution of the Bear Island

Trough Mouth Fan. *Global and Planetary Change*, **12,** 309-330.

LABERG, J.S. & VORREN, T.O. (2000) The Trænadjupet Slide, Offshore Norway - Morphology, Evacuation and Triggering Mechanisms. *Marine Geology*, **171,** 95-114.

LABERG, J.S., VORREN, T.O., DOWDESWELL, J.A., KENYON, N.H. & TAYLOR, J. (2000) The Andøya Slide and the Andøya Canyon, North-Eastern Norwegian–Greenland Sea. *Marine Geology*, **162,** 259-275.

LABERG, J.S., DAHLGREN, K.I.T., VORREN, T.O., HAFLIDASON, H. & BRYN, P. (2001) Seismic Analyses of Cenozoic Contourite Drift Development in the Northern Norwegian Sea. *Marine Geophysical Researches*, **22,** 401-416.

LABERG, J.S., VORREN, T.O., MIENERT, J., BRYAN, P. & LIEN, R. (2002) The Trænadjupet Slide: A Large Slope Failure Affecting the Continental Margin of Norway 4,000 Years Ago. *Geo-Marine Letters*, **22,** 19-24.

LABERG, J.S., VORREN, T.O., MIENERT, J., HAFLIDASON, H. & BRYN, P. (2003) Preconditions Leading to the Holocene Trænadjupet Slide Offshore Norway. In: *Submarine Mass Movements and Their Consequences* (Ed. by J. Locat & J. Mienert), 247–254. Kluwer Academic Publishing.

LABERG, J.S. & CAMERLENGHI, A. (2008) The Cignificance of Contourites for Submarine Slope Stability. In: *Contourites, Developments in Sedimentology* (Ed. by M. Rebesco & A. Camerlenghi), **60**, 537-556. Elsevier, Netherlands.

LABERG, J.S., ANDREASSEN, K., KNIES, J., VORREN, T.O. & WINSBORROW, M. (2010) Late Pliocene - Pleistocene Development of the Barents Sea Ice Sheet. *Geology*, **38,** 107-110.

LABERG, J.S., ANDREASSEN, K. & VORREN, T.O. (2012) Late Cenozoic Erosion of the High-Latitude Southwestern Barents Sea Shelf Revisited. *GSA Bulletin*, **124,** 77-88.

LEE, H.J., LOCAT, J., DESGAGNES, P., PARSONS, J.D., MCADOO, B.G., ORANGE, D.L., PUIG, P., WONG, F.L., DARTNELL, P. & BOULANGER, E. (2007) Submarine Mass Movements on Continental Margins. In: *Continental Margin Sedimentation. From Sediment Transport to Sequence Stratigraphy* (Ed. by C. A. Nittrouer, J. A. Austin, M. E. Field, J. H. Kravitz, J. P. M. Syvitski & P. L. Wiberg), 215-274. Special Publication N 37 of the International Association of Sedimentologists.

LEYNAUD, D., MIENERT, J. & VANNESTE, M. (2009) Submarine Mass Movements on Glaciated and Non-Glaciated European Continental Margins: A Review of Triggering Mechanisms and Preconditions to Failure. *Marine and Petroleum Geology*, **26,** 618-632.

LINDBERG, B., LABERG, J.S. & VORREN, T.O. (2004) The Nyk Slide—Morphology, Progression, and Age of a Partly Buried Submarine Slide Offshore Northern Norway. *Marine Geology*, **213,** 277-289.

LUCCHI, R.G., PEDROSA, M.T., CAMERLENGHI, A., URGELES, R., MOL, B.D. & REBESCO, M. (2012) Recent Submarine Landslides on the Continental Slope of Storfjorden and Kveithola Trough-Mouth Fans (North West Barents Sea). In: *Submarine Mass Movements and Their Consequences* (Ed. by Y. Yamada, K. Kawamura, K. Ikehara, Y. Ogava, R. Urgeles, D. Mosher, J.

Chaytor & M. Strasser), **31**, 735-745. Springer.

LUNDIN, E. & DORE, A.G. (2002) Mid-Cenozoic Post-Break Deformation in the 'Passive' Margins Bordering the Norwegian-Greenland Sea. *Marine and Petroleum Geology*, **19,** 79-83.

MITCHUM, R.M., VAIL, P.R. & SANGREE, J.B. (1977) Seismic Stratigraphy and Global Changes of Sea Level, Part 6: Stratigraphic Interpretation of Seismic Reflection Patterns in Depositional Sequences. In: *Seismic Stratigraphy--Applications to Hydrocarbon Exploration* (Ed. by C. E. Payton), 117-133. AAPG Memoir 26.

MOSAR, J., LEWIS, G. & TORSVIK, T.H. (2002) North Atlantic Sea-Floor Spreading Rates: Implications for the Tertiary Development of Inversion Structures of the Norwegian - Greenland Sea. *Journal of the Geological Society, London*, **159,** 503-515.

MOSCARDELLI, L. & WOOD, L. (2008) Newclassification Systemformass Transport Complexes in Offshoretrinidad. *Basin Research*, **20,** 73-98.

MOSHER, D.C., MORAN, K. & R.N., H. (1994) Late Quaternary Sediment, Sediment Mass Flow Processes and Slope Stability on the Scotian Slope, Canada. *Sedimentology*, **41,** 1039-1061.

MOSHER, D.C., MOSCARDELLI, L., SHIPP, C., CHAYTOR, J., BAXTER, C., LEE, H. & URGELES, R. (2010) Submarine Mass Movements and Their Consequences. *4th International Symposium, in Advances in Natural and Technological Hazards Research***,** 1-8.

MULDER, T. & COCHONAT, P. (1996) Classification of Offshore Mass Movements. *Journal of Sedimentary Research*, **66,** 43-57.

PRIOR, D.B., BORNHOLD, B.D. & JOHNS, M.W. (1984) Depositional Characteristics of a Submarine Debris Flow. *The Journal of Geology*, **92,** 707-727.

REBESCO, M. & STOW, D. (2001) Seismic Expression of Contourites and Related Deposits: A Preface. *Marine Geophysical Researches*, **22,** 303-308.

REBESCO, M., PEDROSA, M.T., CAMERLENGHI, A., LUCCHI, R.G., SAULI, C., MOL, B.D., MADRUSSANI, G., URGELES, R., ROSSI, G. & BOHM, G. (2012) One Million Years of Climatic Generated Landslide Events on the Northwestern Barents Sea Continental Margin. In: *Submarine Mass Movements and Their Consequences* (Ed. by Y. Yamada, K. Kawamura, K. Ikehara, Y. Ogava, R. Urgeles, D. Mosher, J. Chaytor & M. Strasser), **31**, 747-756. Springer.

REBESCO, M., LABERG, J.S., PEDROSA, M.T., CAMERLENGHI, A., LUCCHI, R.G., ZGUR, F. & WARDELL, N. (2014) Onset and Growth of Trough-Mouth Fans on the North-Western Barents Sea Margin: A Stack of Extreme Events. *submitted to Quaternary Science Reviews*, **92,** 227-234.

SMELROR, M. (1999) Pliocene–Pleistocene and Redeposited Dinoflagellate Cysts from the Western Svalbard Margin (Site

986): Biostratigraphy, Paleoenvironments and Sediment Provenance. *Proceedings of the Ocean Drilling Program, Scientific Results*. M. E. Raymo, E. Jansen, P. Blum & T. D. Herbert. **162,** 83-87.

SOLHEIM, A., FALEIDE, J.I., ANDERSEN, E.S., ELVERHOI, A., FORSBERG, C.F., VANNESTE, K.,

UENZELMANN-NEBEN, G. & CHANNELL, J.E.T. (1998) Late Cenozoic Seismic Stratigraphy and Glacial Geological Development of the East Greenland and Svalbard-Barents Sea Continental Margins. *Quaternary Science Reviews*, **17,** 155-184.

SOLHEIM, A., BERG, K., FORSBERG, C.F. & BRYN, P. (2005) The Storegga Slide Complex: Repetitive Large Scale Sliding with Similar Cause and Development. *Marine and Petroleum Geology*, **22,** 97-107.

SULTAN, N., COCHONAT, P., CANALS, M., CATTANEO, A., DENNIELOU, B., HAFLIDASON, H., LABERG, J.S., LONG, D., MIENERT, J., TRINCARDI, F., URGELES, R., VORREN, T. & WILSON, C. (2004) Triggering Mechanisms of Slope Instability Processes and Sediment Failures on Continental Margins: A Geotechnical Approach. *Marine Geology*, **213,** 291-321.

SæTTEM, J., POOLE, D.A.R., ELLINGSEN, K.L. & SEJRUP, H.P. (1992) Glacial Geology of Outer Bjørnøyrenna, Southwestern Barents Sea. *Marine Geology*, **103,** 15-51.

SæTTEM, J., BUGGE, T., FANAVOLL, S., GOLL, R.M., MøRK, A., MøRK, M.B.E., SMELROR, M. & VERDENIUS, J.G. (1994) Cenozoic Margin Development and Erosion of the Barents Sea: Core Evidence from Southwest of Bjørnøya. *Marine Geology*, **118,** 257-281.

TALWANI, M. & ELDHOLM, O. (1977) Evolution of the Norwegian-Greenland Sea. *Geological Society of America Bulletin*, **88,** 969-999.

VAIL, P.R., MITCHUM, R.M., TODD, R.G., WIDMIER, J.M., THOMPSON, S., SANGREE, J.B., BUBB, J.N. & HATLEDID, W.G. (1977) Seismic Stratigraphy and Global Changes in Sea Level. In: *Seismic Stratigraphy - Applications to Hydrocarbon Exploration* (Ed. by C. E. Payton), **26**, 49-2012. American Association of Petroleum Geologists Memoir.

VANNESTE, M., MIENERT, J. & BUNZ, S. (2006) The Hinlopen Slide: A Giant, Submarine Slope Failure on the Northern Svalbard Margin, Arctic Ocean. *Earth and Planetary Science Letters*, **245,** 373-388.

VEEKEN, P.C.H. & MOERKERKEN, B. (2013) *Seismic Stratigraphy and Depositional Facies Models*. EAGE Publication bv, The Netherlands.

VORREN, T., RICHARDSEN, G., KNUTSEN, S.M. & HENRIKSEN, E. (1991) Cenozoic Erosion and Sedimentation in the Western Barents Sea. *Marine and Petroleum Geology*, **8,** 317-340.

VORREN, T.O., LEBESBYE, E., ANDREASSEN, K. & LARSEN, K.B. (1989) Glacigenic Sediments on a Passive Continental Margin as Exemplified by the Barents Sea. *Marine Geology*, **85,** 251-272.

VORREN, T.O. & LABERG, J.S. (1997) Trough Mouth Fans - Palaeoclimate and Ice-Sheet Monitors. *Quaternary Science Reviews*, **16,** 865-881.

VORREN, T.O., LABERG, J.S., BLAUME, F., DOWDESWELL, J.A., KENYON, N.H., MIENERT, J., RUMOHR, J. & WERNER, F. (1998) The Norwegian-Greenland Sea Continental Margins; Morphology and Late Quaternary Sedimentary Processs and Environment. *Quaternary Science Reviews.*, **17,** 273-302.

Figure captures

Figure 1A Bathymetric map of the western Barents Sea-Svalbard passive continental margin with location of the study area indicated (within the yellow rectangle) and distribution of large-scale Trough Mouth Fans (TMF) along the margin. The map was made in the Generic Mapping Tools (GMT), and the source of the bathymetry and land topography data are from IBCAO (International Bathymetric Chart of the Ocean). **(B)** Distribution of 2D seismic datasets used during this study. Profile A is located in proximity to the ODP Site 986.

Figure 2 (A) Bathymetric map of the western Barents Sea-Svalbard margin with tectonic elements, indicated by dark grey lines, shows a distribution of submarine slides along the NE Atlantic margin: (1) mapped areal extent of the slide debrite 1 (SFU1); (2) mapped areal extent of the slide debrite 3 (SFU3); (3) shallow landslide 1 (LS-1) (Rebesco et al., 2012); (4) Bjørnøya fan mega-slide III (Hjelstuen et al., 2007); (5) Bjørnøya fan mega-slide II (Hjelstuen et al., 2007); (6) Bjørnøya fan mega-slide I (Hjelstuen et al., 2007); (7) Bjørnøyrenna Slide (Laberg and Vorren, 1993; 1996); (8) Slide A (Laberg and Vorren, 1996); (9) Slide B (Laberg and Vorren, 1996); (10) Andøya Slide (Laberg et al., 2000); (11) Trænadjupet Slide (Laberg et al., 2002); (12) Nyk Slide (Lindberg et al., 2004). The Figure is partly modified from Hjelstuen et al., 2007. See Table 1 for details about indicated submarine slides. Distribution of the Spitsbergen Shear Zone (SSZ) boundaries is outlined between two white lines. **(B)** Time-thickness map of the slide debrite 1 (SFU1). Red dashed line indicates a potential larger areal extent of the slide debrite 1. **(C)** Time-thickness map of the slide debrite 3 (SFU3). Pink dashed line indicates a potential larger areal extent of the slide debrite 3.

Figure 3 Examples of seismic facies units observed within the depositional sequence GI (2.7 – 1.5 Ma): **(A)** Chaotic; **(B)** Transparent/reflection-free; **(C)** Parallel; **(D)** Subparallel; **(E)** Contorted.

Figure 4 (A-B) Uninterpreted and interpreted vertical seismic section across the south-western Svalbard continental margin, showing location of the reflectors R7, R6, R5 and distribution of the submarine slide debrite 1 (SFU1) characterized by chaotic to reflection-free seismic facies. Location of the vertical seismic section is indicated by a red line in the upper left corner on Figure 4A. **(C)** Contorted seismic facies between the reflectors R5 and R6 indicating contouritic deposits. Similar contorted seismic facies are observed in the seismic-stratigraphic interval below the reflector R7 and the interval between reflectors R7 and R6. **(D)** Note that the lower boundary of the submarine slide debrite 1 (SFU1) is seen as a strong reflection, which is parallel to the underlying reflections. Note the upper boundary of SFU1 is formed by ridges.

Figure 5 (A) Vertical seismic section shows changes in seismic reflection pattern along the NW Barents Sea margin. Large-scale submarine slide debrites SFU1-5 are highlighted within the interval between the regional reflectors R6 and R7. **(B)** Uninterpreted part of the vertical seismic section showing a submarine slide debrite 1 (SFU1) characterized by chaotic to reflection-free seismic facies. **(C)** Uniterpreted part of the vertical seismic sections showing seismic slide debrites 2 to 5 (SFU2-5) separated by continuous high-amplitude reflections.

Figure 6 (A) Synthetic seismogram for the ODP Site 986 modified from Jansen et al. (1996). It is plotted in twt below sea-floor. Locations of the seismic reflectors R5 and R6 (black continuous line) were taken from the original figure of Jansen et al. (1996) with the synthetic seismogram. Location of the seismic reflector R7 (black dashed line) were identified based on the depth information (in twt) seen in the Table 2 taken from the Jansen et al. (1996) study. **(B)** Profile A is located in proximity to the ODP Site 986 on the SW Svalbard margin. For location also see Fig. 4B. The major regional reflectors R7 (oldest), R6 and R5 (youngest) are indicated. Precise depth in two-way travel time (twt) in seconds for the reflectors R7-R1 is indicated in Table 2.

Figure 7 (A-B) Vertical seismic section shows that reflector R5 and R6 indicating regional erosional surfaces. Location is indicated in the upper left corner by a red line and on Figure 7C. **(C)** Time-thickness map of the depositional sequence GI between reflectors R5 and R7. Red polygon indicates an outline of the seismic facies unit 1 (SFU1). Blue polygon indicates an outline of the seismic facies unit 3 (SFU3).

Figure 8 (A-B) Along slope oriented vertical seismic section showing chaotic to reflection-free seismic facies within the seismic facies unit 1 (SFU1) and its relationship to a prominent palaeo-scar upslope. Reflectors R5, R6 and R7 are indicated. Location of the vertical seismic section is shown in the upper left corner by a red line. **(B)** Vertical seismic section showing medium- to high-amplitude continuous, parallel seismic reflections (contouritic drift?) onlaping the palaeo-scar.

Figure 9 (A-B) Uninterpreted and interpreted vertical seismic section shows a distribution of four chaotic to reflection-free seismic facies units named as SFU2, SFU3, SFU4 and SFU5 between the two regional reflectors R6 and R7. **(C)** Note that the seismic facies units 2-5 are separated by continuous high-amplitude reflections. The seismic facies units are formed by ridges and thrusts. **(D)** Vertical seismic section shows a potential palaeo-slide scar.

Figure 10 Timing and location of large-scale submarine slides formed during the Late Pliocene-Pleistocene along the Svalbard-Barents Sea margin.

Figure 11 Conceptual model illustrating formation of the large-scale submarine slide debrite 1 (SFU1) in the north of the study area. **(A)** Original cross-section before the formation of the submarine slide debrite 1 (SFU1). **(B)** Formation of the SFU1. **(C)** Deposition of contourites above the SFU1.

Table 1 "Minimum" estimated areas and volumes of the submarine slide debrites 1 (SFU1) and 3 (SFU3), which are compared with other submarine slides along the NE Atlantic margin. The table is partly modified from Hjelstuen et al., 2007. See Figure 2A for location.

Table 2 Seismic reflectors R1-R7 penetrated by the ODP Site 986. Information about their age estimate is also provided.

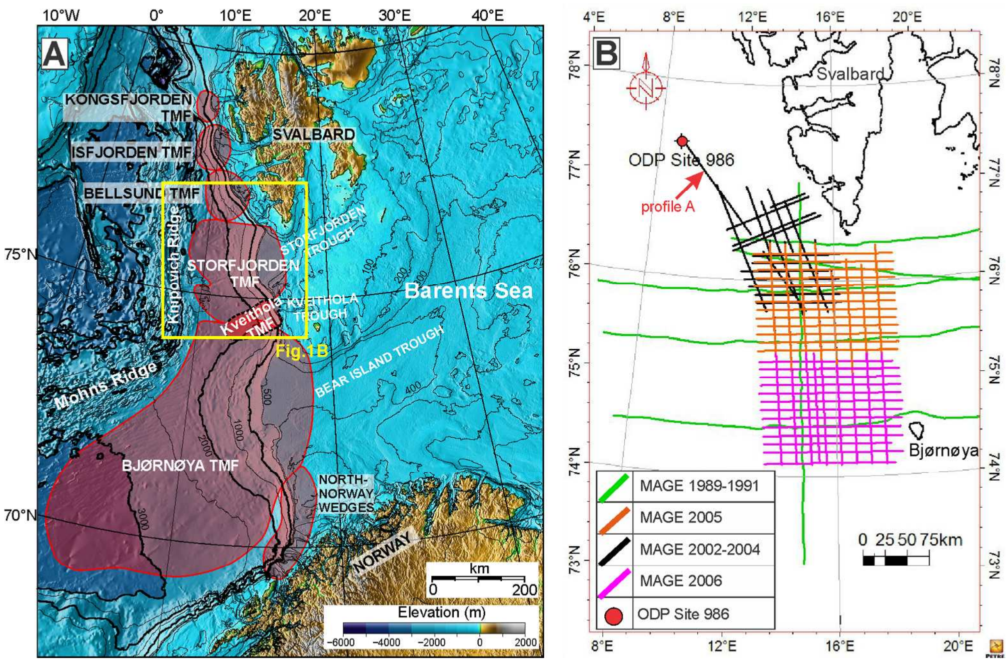

Figure 1A Bathymetric map of the western Barents Sea-Svalbard passive continental margin with location of the study area indicated (within the yellow rectangle) and distribution of large-scale Trough Mouth Fans (TMF) along the margin. The map was made in the Generic Mapping Tools (GMT), and the source of the bathymetry and land topography data are from IBCAO (International Bathymetric Chart of the Ocean). (B) Distribution of 2D seismic datasets used during this study. Profile A is located in proximity to the ODP Site 986.

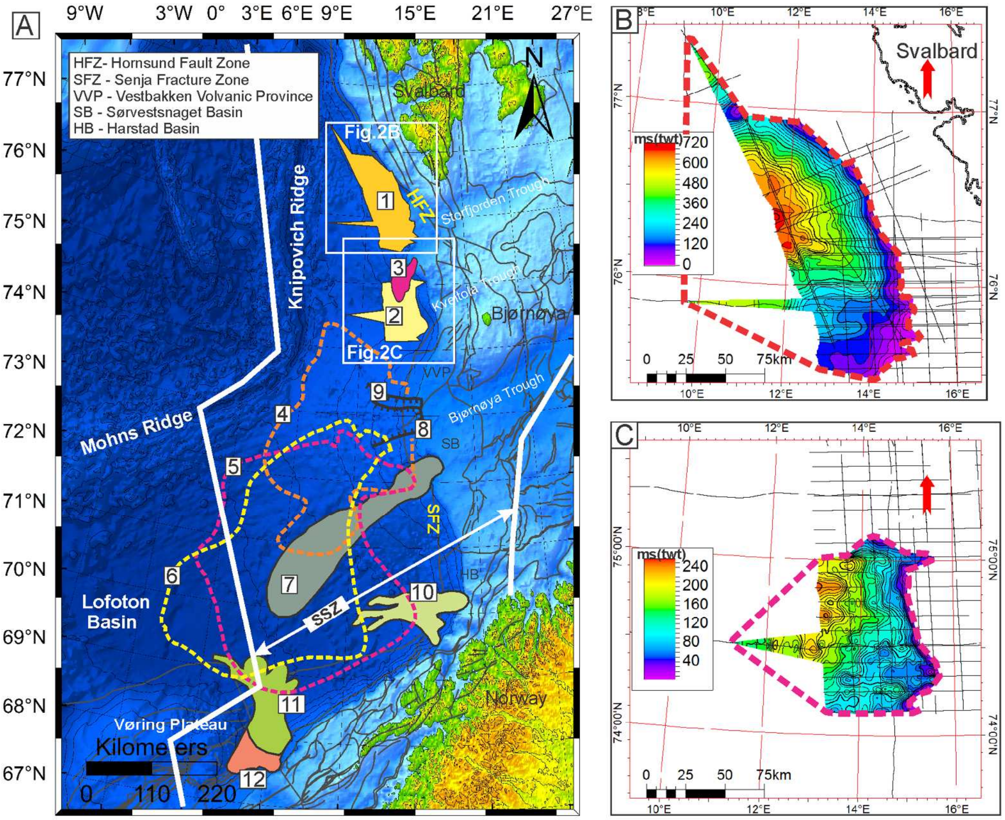

Figure 2 (A) Bathymetric map of the western Barents Sea-Svalbard margin with tectonic elements, indicated by dark grey lines, shows a distribution of submarine slides along the NE Atlantic margin: (1) mapped areal extent of the slide debrite 1 (SFU1); (2) mapped areal extent of the slide debrite 3 (SFU3); (3) shallow landslide 1 (LS-1) (Rebesco et al., 2012); (4) Bjørnøya fan mega-slide III (Hjelstuen et al., 2007); (5) Bjørnøya fan mega-slide II (Hjelstuen et al., 2007); (6) Bjørnøya fan mega-slide I (Hjelstuen et al., 2007); (7) Bjørnøyrenna Slide (Laberg and Vorren, 1993; 1996); (8) Slide A (Laberg and Vorren, 1996); (9) Slide B (Laberg and Vorren, 1996); (10) Andøya Slide (Laberg et al., 2000); (11) Trænadjupet Slide (Laberg et al., 2002); (12) Nyk Slide (Lindberg et al., 2004). The Figure is partly modified from Hjelstuen et al., 2007. See Table 1 for details about indicated submarine slides. Distribution of the Spitsbergen Shear Zone (SSZ) boundaries is outlined between two white lines. (B) Time-thickness map of the slide debrite 1 (SFU1). Red dashed line indicates a potential larger areal extent of the slide debrite 1. (C) Time-thickness map of the slide debrite 3 (SFU3). Pink dashed line indicates a potential larger areal extent of the slide debrite 3.

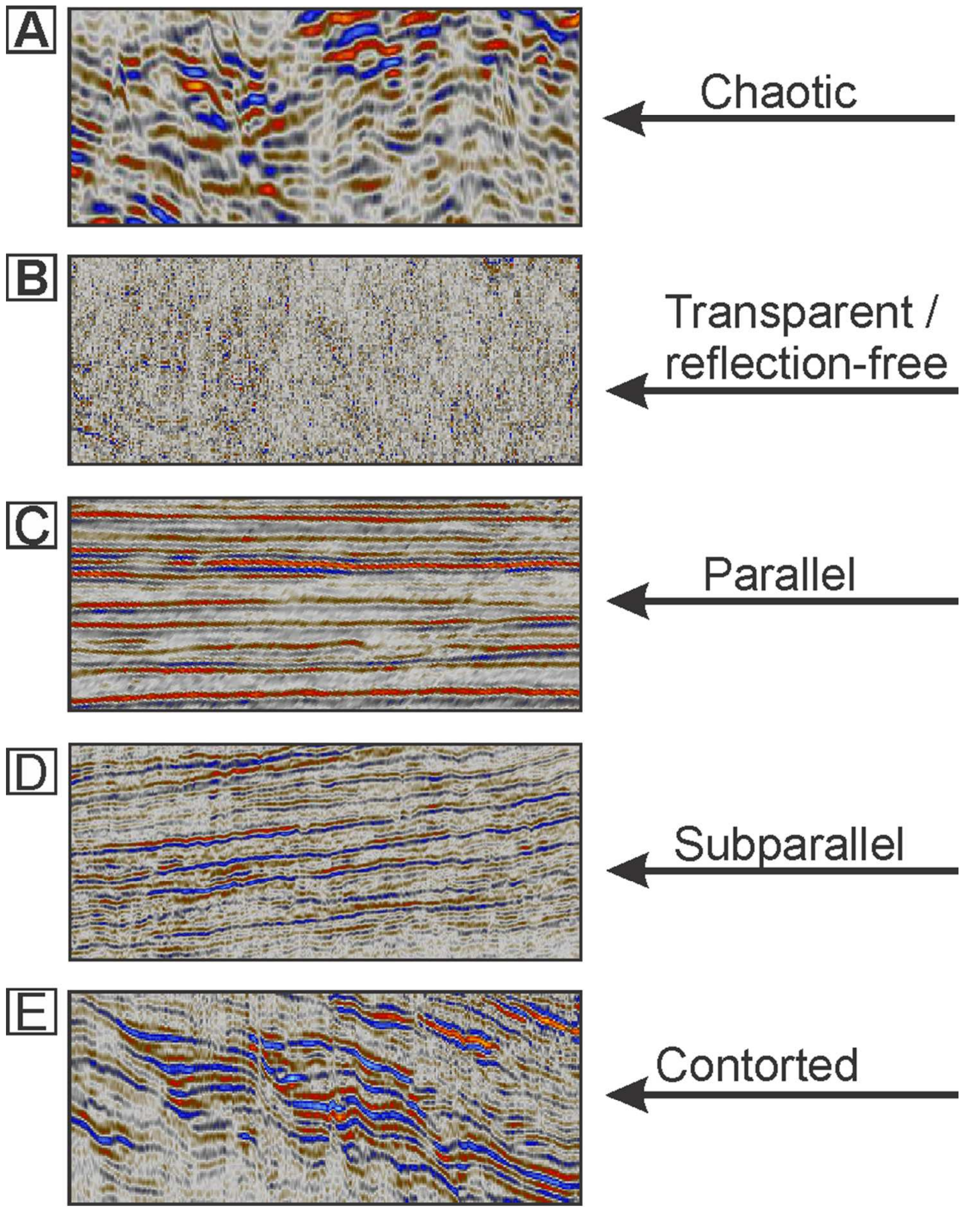

Figure 3 Examples of seismic facies units observed within the depositional sequence GI (2.7 – 1.5 Ma): (A) Chaotic; (B) Transparent/reflection-free; (C) Parallel; (D) Subparallel; (E) Contorted.

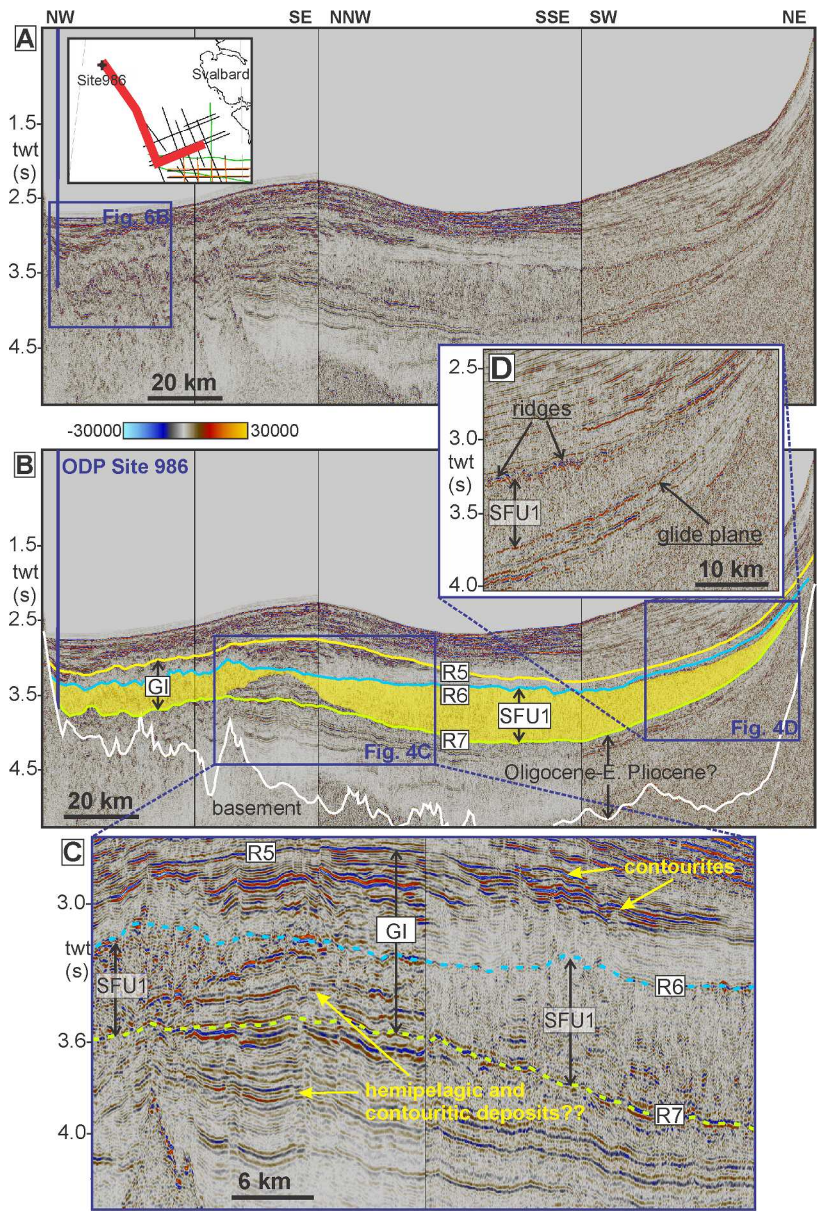

Figure 4 (A-B) Uninterpreted and interpreted vertical seismic section across the south-western Svalbard continental margin, showing location of the reflectors R7, R6, R5 and distribution of the submarine slide debrite 1 (SFU1) characterized by chaotic to reflection-free seismic facies. Location of the vertical seismic section is indicated by a red line in the upper left corner on Figure 4A. (C) Contorted seismic facies between the reflectors R5 and R6 indicating contouritic deposits. Similar contorted seismic facies are observed in the seismic-stratigraphic interval below the reflector R7 and the interval between reflectors R7 and R6. (D) Note that the lower boundary of the submarine slide debrite 1 (SFU1) is seen as a strong reflection, which is parallel to the underlying reflections. Note the upper boundary of SFU1 is formed by ridges.

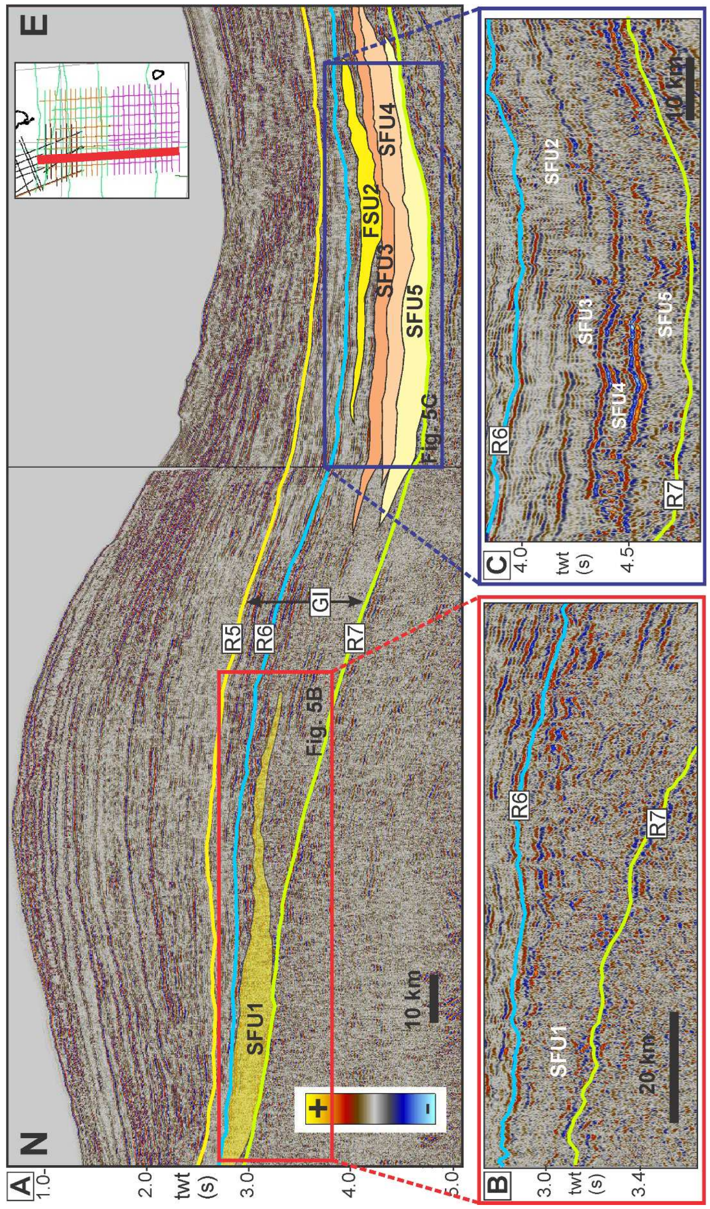

Figure 5 (A) Vertical seismic section shows changes in seismic reflection pattern along the NW Barents Sea margin. Large-scale submarine slide debrites SFU1-5 are highlighted within the interval between the regional reflectors R6 and R7. (B) Uninterpreted part of the vertical seismic section showing a submarine slide debrite 1 (SFU1) characterized by chaotic to reflection-free seismic facies. (C) Uniterpreted part of the vertical seismic sections showing seismic slide debrites 2 to 5 (SFU2-5) separated by continuous high-amplitude reflections.

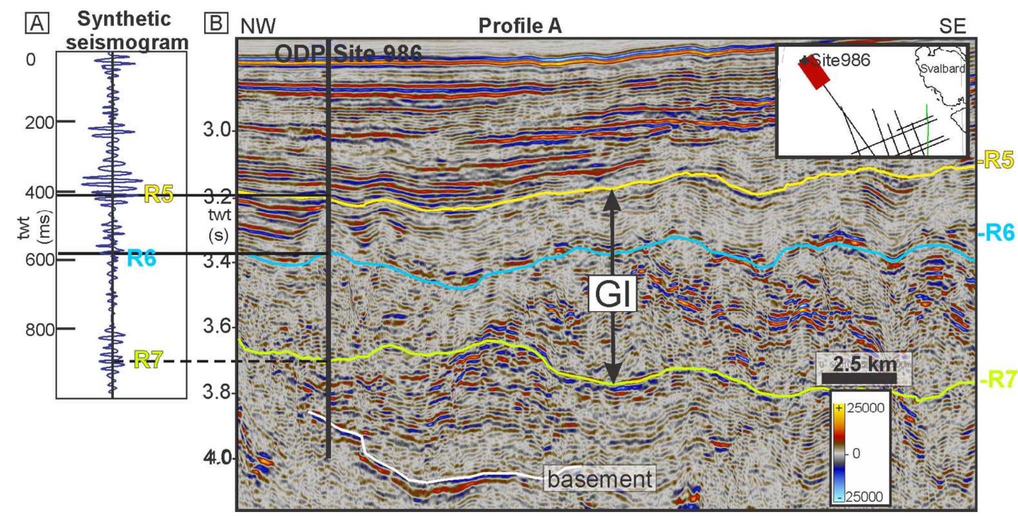

Figure 6 (A) Synthetic seismogram for the ODP Site 986 modified from Jansen et al. (1996). It is plotted in twt below sea-floor. Locations of the seismic reflectors R5 and R6 (black continuous line) were taken from the original figure of Jansen et al. (1996) with the synthetic seismogram. Location of the seismic reflector R7 (black dashed line) were identified based on the depth information (in twt) seen in the Table 2 taken from the Jansen et al. (1996) study. (B) Profile A is located in proximity to the ODP Site 986 on the SW Svalbard margin. For location also see Fig. 4B. The major regional reflectors R7 (oldest), R6 and R5 (youngest) are indicated. Precise depth in two-way travel time (twt) in seconds for the reflectors R7-R1 is indicated in Table 2.

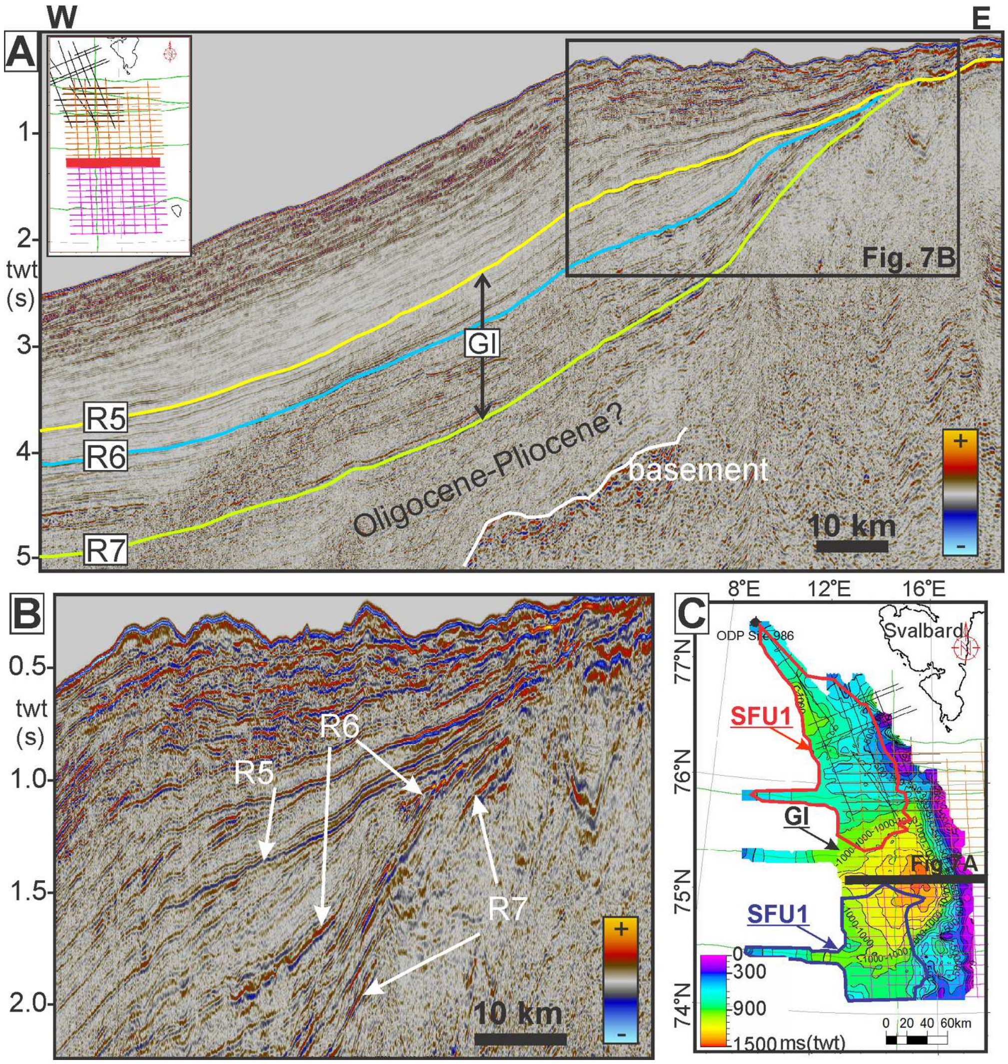

Figure 7 (A-B) Vertical seismic section shows that reflector R5 and R6 indicating regional erosional surfaces. Location is indicated in the upper left corner by a red line and on Figure 7C. (C) Time-thickness map of the depositional sequence GI between reflectors R5 and R7. Red polygon indicates an outline of the seismic facies unit 1 (SFU1). Blue polygon indicates an outline of the seismic facies unit 3 (SFU3).

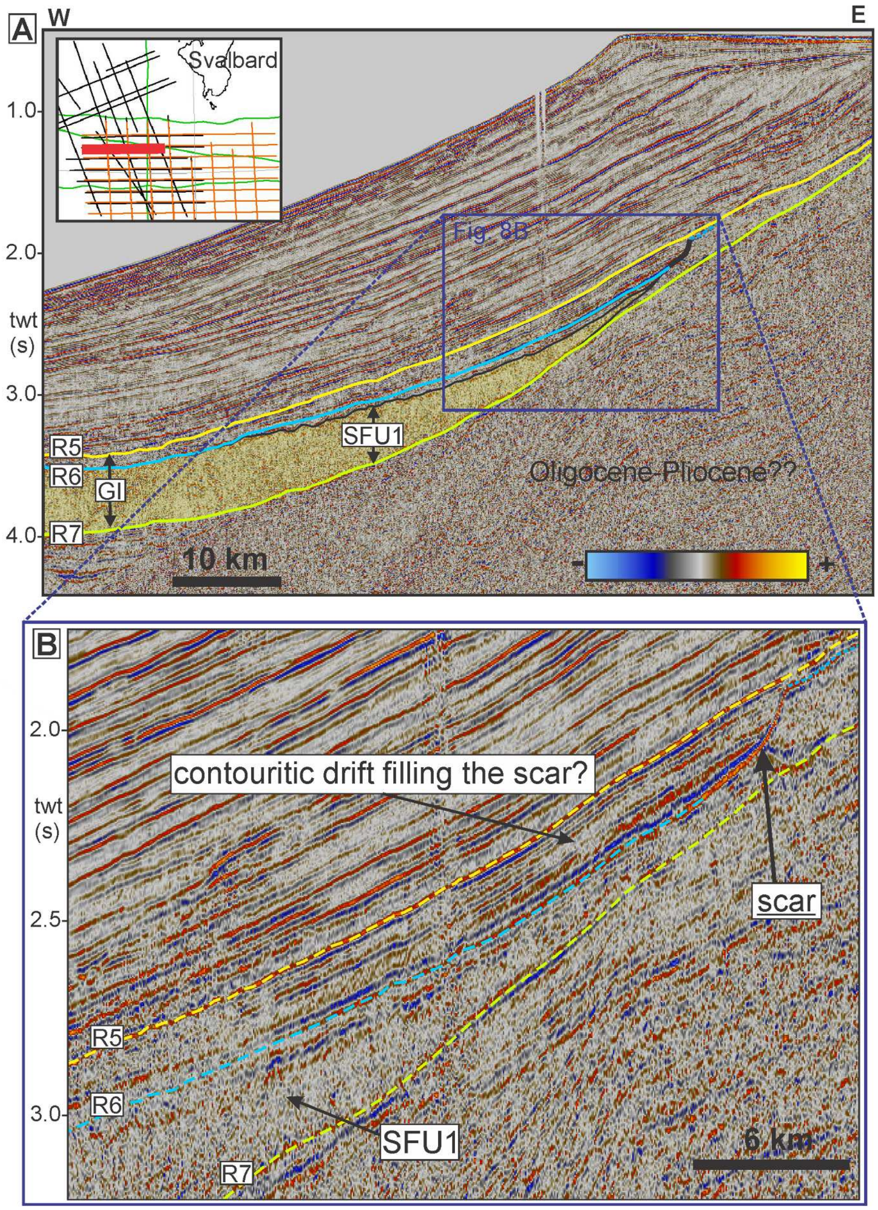

Figure 8 (A-B) Along slope oriented vertical seismic section showing chaotic to reflection-free seismic facies within the seismic facies unit 1 (SFU1) and its relationship to a prominent palaeo-scar upslope. Reflectors R5, R6 and R7 are indicated. Location of the vertical seismic section is shown in the upper left corner by a red line. (B) Vertical seismic section showing medium- to high-amplitude continuous, parallel seismic reflections (contouritic drift?) onlaping the palaeo-scar.

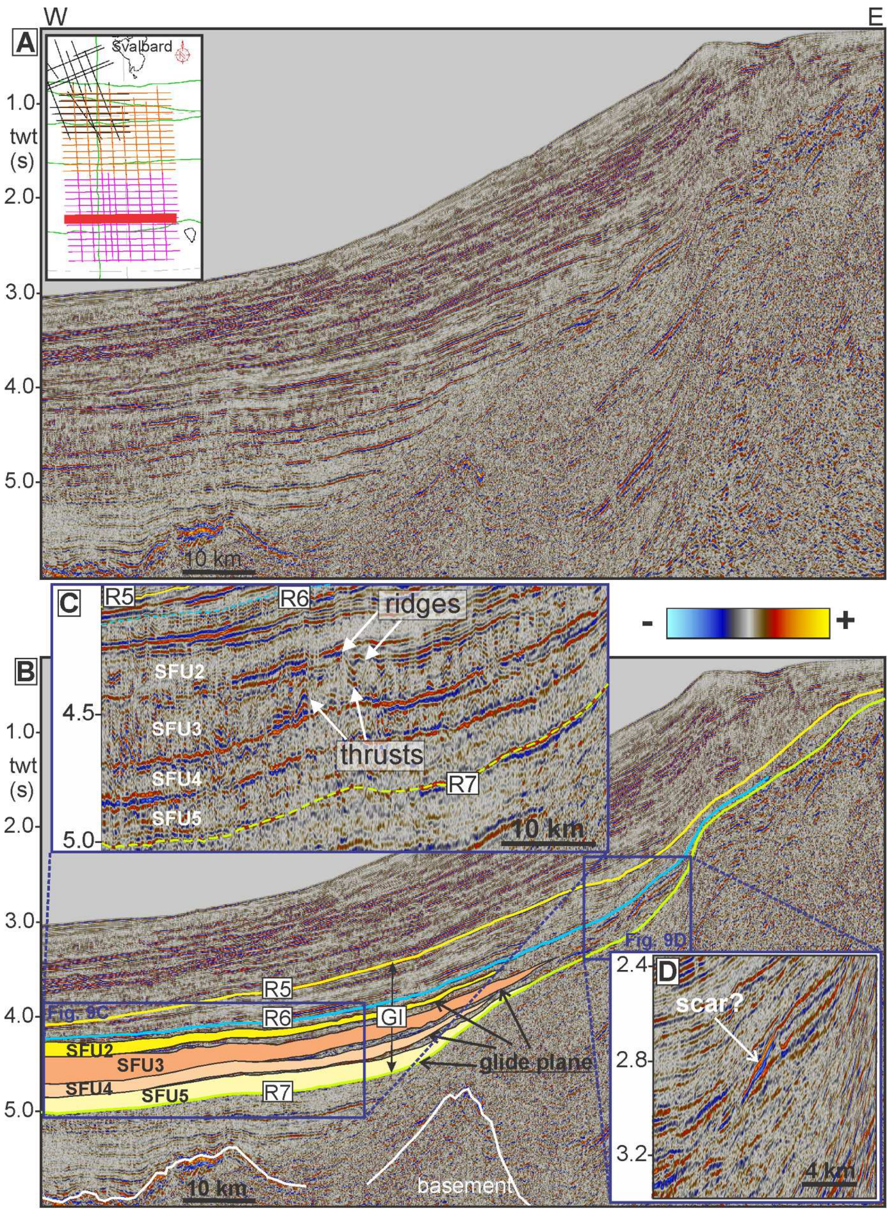

Figure 9 (A-B) Uninterpreted and interpreted vertical seismic section shows a distribution of four chaotic to reflection-free seismic facies units named as SFU2, SFU3, SFU4 and SFU5 between the two regional reflectors R6 and R7. (C) Note that the seismic facies units 2-5 are separated by continuous high-amplitude reflections. The seismic facies units are formed by ridges and thrusts. (D) Vertical seismic section shows a potential palaeo-slide scar.

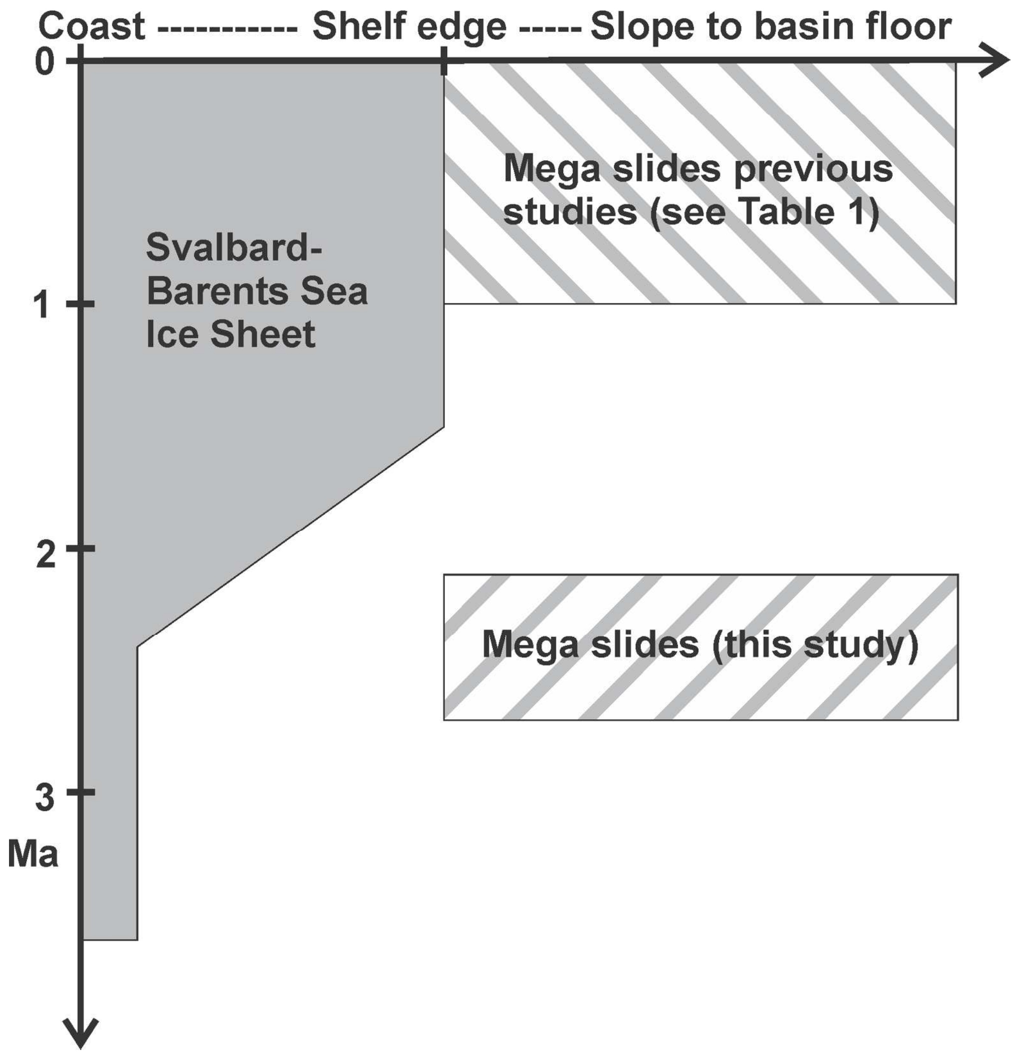

Figure 10 Timing and location of large-scale submarine slides formed during the Late Pliocene-Pleistocene along the Svalbard-Barents Sea margin.

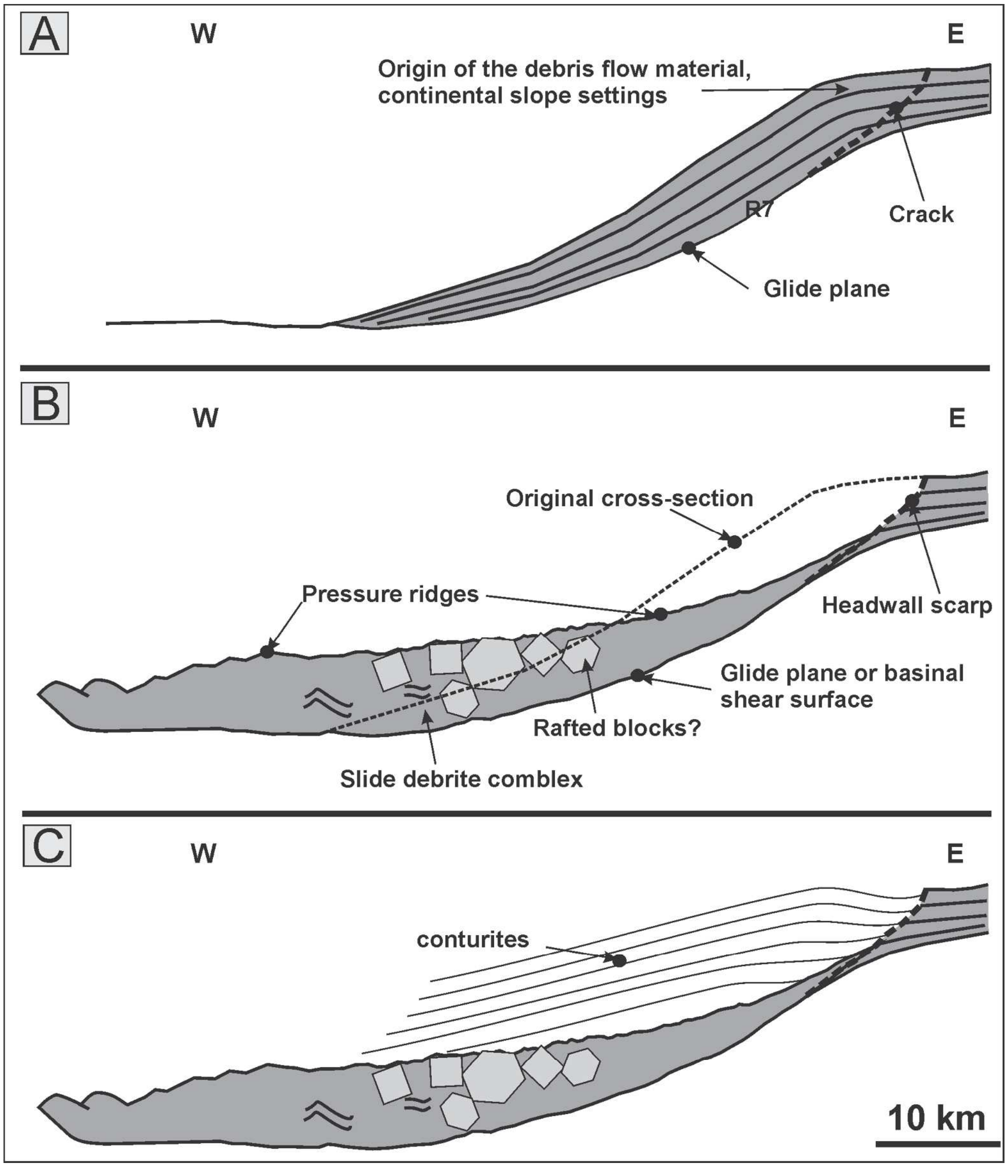

Figure 11 Conceptual model illustrating formation of the large-scale submarine slide debrite 1 (SFU1) in the north of the study area. (A) Original cross-section before the formation of the submarine slide debrite 1 (SFU1). (B) Formation of the SFU1. (C) Deposition of contourites above the SFU1.

Slide	Area ($\times10^3km^2$)	Volume ($\times10^3km^3$)	Age	Reference
Slide debrite 1	10,7	> 4,1	2.7-2.1 Ma	This study
Slide debrite 3	7,04	> 1,1	2.7-2.1 Ma	This study
Bjørnøya fan mega-slide 1	115	25,5	0.78-1.0 Ma	Hjelstuen et al., 2007
Bjørnøya fan mega-slide 2	120	24,5	0.5-0.78 Ma	Hjelstuen et al., 2007
Bjørnøya fan mega-slide 3	66	11,6	0.2-0.5 Ma	Hjelstuen et al., 2007
Landslide 1 (LS-1)	1,1		ca. 70 ka	Lucchi et al. 2012
Slide A	12	5,1	0.5-0.6 Ma	Laberg and Vorren, 1996
Storegga Slide	95	<3,2	0.0072 Ma	Haflidason et al., 2005
Bjørnøyrenna Slide	12,5	1,1	0.2-0.3 Ma	Laberg and Vorren, 1993;1996
Trænadjupet Slide	14,1	0,9	0.004 Ma	Laberg et al., 2002
Andøya Slide	9,7		Holocene	Laberg et al., 2000
Nyk Slide	>2.2		0.0163 Ma	Lindberg et al., 2004

Table 1 "Minimum" estimated areas and volumes of the submarine slide debrites 1 (SFU1) and 3 (SFU3), which are compared with other submarine slides along the NE Atlantic margin. The table is partly modified from Hjelstuen et al., 2007. See Figure 2A for location.

Reflector	Depth in two-way travel time (twt) (Jansen et al., 1996)	Depth in twt; this study	Estimated age (Ma) (Rebesco et al., 2014)	Age estimate (Ma) (e.g. Knies et al., 2009)
Sea-floor	2.885 s	2.785 s		
R1	2.92 s	2.82 s	0.2	~0.2
R2	2.97 s	2.87 s	0.4	~0.5
R3	3.04 s	2.94 s	0.75	~0.78
R4	3.1 s	3.00 s	1.1	~0.99
R4A	3.17 s	3.07 s	1.3	
R5	3.28 s	3.18 s	1.5	(1.3)-1.5
R6	3.465 s	3.36 s	2.1	(1.6) 1.7
R7	3.755 s	3.75 s		~2.7
Basement	~3.985 s	3.885 s		

Table 2 Seismic reflectors R1-R7 penetrated by the ODP Site 986. Information about their age estimate is also provided.